

FAR INFRARED SPECTRA AND THEIR APPLICATION TO
SELECTED PROBLEMS OF MOLECULAR ENERGETICS

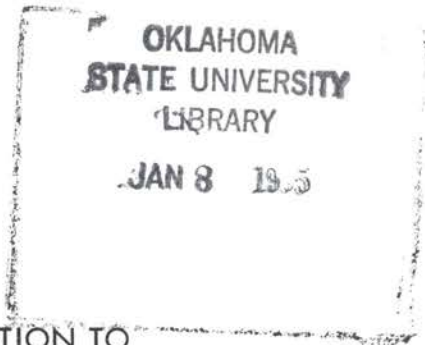
By

Gene A. Crowder

Bachelor of Science
Central State College
Edmond, Oklahoma
1958

Master of Science
University of Florida
Gainesville, Florida
1961

Submitted to the Faculty of the Graduate School of
the Oklahoma State University
in partial fulfillment of the requirements
for the degree of
DOCTOR OF PHILOSOPHY
August, 1964



FAR INFRARED SPECTRA AND THEIR APPLICATION TO
SELECTED PROBLEMS OF MOLECULAR ENERGETICS

Thesis Approved:

George Gorin

Thesis Adviser

J. Paul Devlin

W. Lewis

Clemens M. Cunningham

Louis P. Varga

M. Boyce

Dean of the Graduate School

ACKNOWLEDGEMENTS

The author wishes to express his deep gratitude to Dr. Donald W. Scott for his constant help and advice in directing this research. The encouragement of Professor George Gorin is appreciated. The assistance of many of the staff members of the Bartlesville Petroleum Research Center of the Bureau of Mines is gratefully acknowledged.

The computer work was done by Dr. F. H. Kruse of the Los Alamos Scientific Laboratory, and the computer programs were supplied by Dr. J. H. Schachtschneider of Shell Development Company. Their assistance is greatly appreciated.

The author is deeply indebted to the Petroleum Research Fund of the American Chemical Society for financial support in the form of a fellowship during the entire period of this work.

Finally, thanks are due Mrs. Mavis Bacon and Mrs. Mignon Faust for typing this thesis.

TABLE OF CONTENTS

Chapter	Page
I. INTRODUCTION	1
II. FAR INFRARED SPECTROSCOPY	4
Spectrophotometer	4
Spectra	5
Frequency Shifts between Liquid and Vapor States	42
Results	43
Discussion	45
Study of Restricted Internal Rotation by Infrared Spectroscopy	47
2-Propanethiol	47
Cyclohexanethiol	49
2,3-Dithiabutane	50
Thiacyclopentane	50
Low Fundamentals	51
III. VIBRATIONAL ANALYSIS BY DIGITAL COMPUTER	53
Methods	53
Tetramethyllead	58
2,4-Dimethyl-3-thiapentane	73
IV. STATISTICAL THERMODYNAMIC APPLICATIONS	79
Tetramethyllead	80
Resolution of the Entropy Discrepancy	80
Thermodynamic Properties	82
2,4-Dimethyl-3-thiapentane	85
Conformational Analysis	85
Thermodynamic Properties	89
BIBLIOGRAPHY	91

LIST OF TABLES

Table	Page
I. Far Infrared Absorption Maxima for 2-Methylthiophene . . .	7
II. Far Infrared Absorption Maxima for 3-Methylthiophene . . .	9
III. Far Infrared Absorption Maxima for 4-Methylpyridine . . .	11
IV. Far Infrared Absorption Maxima for 1-Methylpyrrole . . .	13
V. Far Infrared Absorption Maxima for 1,4-Dimethylbenzene . .	15
VI. Far Infrared Absorption Maxima for 1,4-Difluorobenzene . . .	17
VII. Far Infrared Absorption Maxima for 1,3-Difluorobenzene . . .	19
VIII. Far Infrared Absorption Maxima for 1,2-Difluorobenzene . . .	21
IX. Far Infrared Absorption Maxima for 2,4-Dimethyl-3-thia- pentane	23
X. Far Infrared Absorption Maxima for 2,3-Dithiabutane	25
XI. Far Infrared Absorption Maxima for Thiacyclopentane	27
XII. Far Infrared Absorption Maxima for 2-Propanethiol	29
XIII. Far Infrared Absorption Maxima for Cyclohexanethiol	31
XIV. Far Infrared Absorption Maxima for Tetramethyllead	33
XV. Far Infrared Absorption Maxima for Benzenethiol	35
XVI. Far Infrared Absorption Maxima for Benzotrifluoride	37
XVII. Far Infrared Absorption Maxima for Hexamethyldisiloxane . .	39

LIST OF TABLES (Continued)

Table	Page
XVIII. Far Infrared Absorption Maxima for Piperidine	41
XIX. Wavenumbers for Vapor and Liquid (or Solution) and Extent of Shift	44
XX. Far Infrared Bands of Tetramethyllead Vapor	59
XXI. Observed and Calculated Wavenumbers of Tetramethyllead . .	67
XXII. Comparison of Force Constants for Tetramethyllead	68
XXIII. Vibrational Assignment for Tetramethyllead	71
XXIV. Potential Energy Distribution for Tetramethyllead	72
XXV. Force Constants for 2,4-Dimethyl-3-thiapentane	77
XXVI. Observed and Calculated Wavenumbers of 2,4-Dimethyl- 3-thiapentane	78
XXVII. The Molal Thermodynamic Properties of Tetramethyllead in the Ideal Gas State	84
XXVIII. Comparison of Observed and Calculated Entropy and Heat Capacity for 2,4-Dimethyl-3-thiapentane	89
XXIX. The Molal Thermodynamic Properties of 2,4-Dimethyl- 3-thiapentane in the Ideal Gas State	90

LIST OF FIGURES

Figure	Page
1. Spectra of 2-Methylthiophene	6
2. Spectra of 3-Methylthiophene	8
3. Spectra of 4-Methylpyridine	10
4. Spectra of 1-Methylpyrrole	12
5. Spectra of 1,4-Dimethylbenzene	14
6. Spectra of 1,4-Difluorobenzene	16
7. Spectra of 1,3-Difluorobenzene	18
8. Spectra of 1,2-Difluorobenzene	20
9. Spectra of 2,4-Dimethyl-3-thiapentane	22
10. Spectra of 2,3-Dithiabutane	24
11. Spectra of Thiacyclopentane	26
12. Spectra of 2-Propanethiol	28
13. Spectra of Cyclohexanethiol	30
14. Spectra of Tetramethyllead	32
15. Spectra of Benzenethiol	34
16. Spectra of Benzotrifluoride	36
17. Spectra of Hexamethyldisiloxane	38

LIST OF FIGURES (Continued)

Figure	Page
18. Spectra of Piperidine	40
19. Internal Coordinates of Tetramethyllead	60
20. Equilibrium Configuration of 2,4-Dimethyl-3-thiapentane	74
21. Potential Function Assumed for Isopropyl Rotation	88

CHAPTER I

INTRODUCTION

In this research project, studies of far infrared spectra that were made possible by recent advances in instrumentation were applied to selected problems in chemical thermodynamics. The thesis consists of two parts. The first part is a survey of a variety of compounds for which it could be anticipated that examination of the far infrared spectra would provide a significant insight into the molecular energetics. The second part describes the utilization of the results for two selected compounds, tetramethyllead and 2,4-dimethyl-3-thiapentane, in detailed statistical thermodynamic analyses that included use of molecular vibrational analysis by digital computer.

Until very recently, far infrared spectroscopy had only rarely been applied to chemical problems. Investigations of fundamental vibrational frequencies in the portion of the spectrum between the microwave region and about 250 cm^{-1} were conducted in the past by Raman instrumentation, except for limited studies with a few "homemade" grating infrared spectrometers. However, the introduction of commercially available far infrared grating spectrometers has opened this region for investigation by infrared instrumentation on a scale that eventually will be comparable with that of Raman spectroscopy. Two reasons for a growing interest

in far infrared spectroscopy are: First, some frequencies that have an intensity too low to be observed in the Raman effect are easily observable in the infrared; and, second, the resolution obtainable in infrared spectra is usually better than that in Raman spectra. Other reasons will become apparent in this report. There are also reasons for continued interest in Raman spectroscopy, the main one being that highly symmetrical molecules usually have vibrations that are infrared inactive but are allowed in the Raman effect.

Transitions between rotational energy levels occur in the far infrared region of the spectrum only for molecules possessing small moments of inertia. The rotational transitions of larger molecules lie entirely in the microwave region, so in this investigation only vibrational (or rotational-vibrational) transitions are of interest. Low internal vibrational frequencies occur in most molecules that are of thermodynamic interest. In general, the fundamental vibrations that give rise to infrared absorption below 250 cm^{-1} are bending or restricted internal rotational modes. These types of vibration are of particular interest in this investigation, but some stretching modes also were observed at higher wavenumbers in the survey, which covered the spectra of eighteen compounds from $50\text{--}70 \text{ cm}^{-1}$ up to 650 cm^{-1} . It has been recently discovered that the low-frequency vibrations are often different in the vapor and liquid states, and it will be shown that this phenomenon has important consequences in calculating thermodynamic properties.

The specific objectives of this research were: first, to investigate the liquid-vapor shifts (or solution-vapor shifts) of low fundamental frequencies in the far infrared spectra of compounds of thermodynamic interest; second, to observe torsional

frequencies in compounds of interest; third, to find fundamental frequencies that do not appear in the Raman effect because of selection rules or unfavorable intensity; and, fourth, to calculate thermodynamic functions, make vibrational assignments, and evaluate structural parameters from calorimetric data for tetramethyllead and 2,4-dimethyl-3-thiapentane, using the results of far infrared studies and normal-coordinate calculations.

The compounds selected for this investigation were ones for which calorimetric data were available, or which were being studied in the Bureau of Mines Thermodynamics Laboratory. Tetramethyllead was selected for a detailed study in order to resolve an entropy discrepancy that had been a puzzle for the past decade. 2,4-Dimethyl-3-thiapentane was selected for the second detailed study because calorimetric data available for the compound made possible a clearer insight into the molecular energetics.

CHAPTER II

FAR INFRARED SPECTROSCOPY

This chapter describes the experimental apparatus, shows the spectra that were obtained, and gives some observations based on the observed spectra.

Spectrophotometer

The spectra were obtained with a Perkin-Elmer Model 301 far infrared spectrophotometer. This is a double beam instrument which covers the infrared region from about 650 to 50 cm^{-1} . Diffraction gratings are used throughout this range as the dispersing elements. Two sources are used to cover the range of the instrument; a water-cooled globalar is used from 650 to about 100 cm^{-1} and a Mercury H4 lamp is used from about 100 to 50 cm^{-1} .

Since water vapor absorbs strongly at many frequencies in the far infrared region, the spectrometer must be purged several times in the course of a single scan. Dry nitrogen gas was used for this purpose. The scan is halted during the purge.

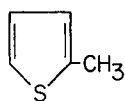
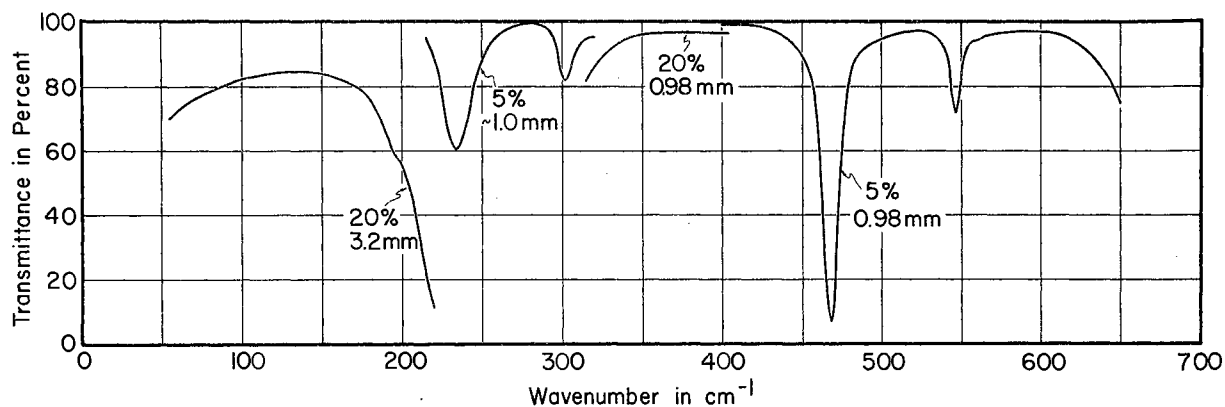
The absorption cells used for obtaining the liquid and solution spectra had cesium bromide windows for the region 650 - 320 cm^{-1} and high density polyethylene windows for the region 320 - 50 cm^{-1} . The change was made at the most convenient point, 320 cm^{-1} , since the filter used to eliminate undesired radiation, as well as the choppers, must be changed at that wavenumber.

The vapor cell was built especially for the Model 301 spectrophotometer, and is made of stainless steel. It contains a system of gold-plated mirrors which can be adjusted to give path lengths from one meter up to six meters. When mounted in the spectrometer, the cell is connected directly to a vacuum system by means of flexible stainless steel tubing, the end of which is attached to a stainless steel o-ring connector.

The spectrometer was calibrated against atmospheric water vapor absorption bands (1,2). The accuracy of the calibration was about $\pm 1 \text{ cm}^{-1}$.

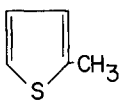
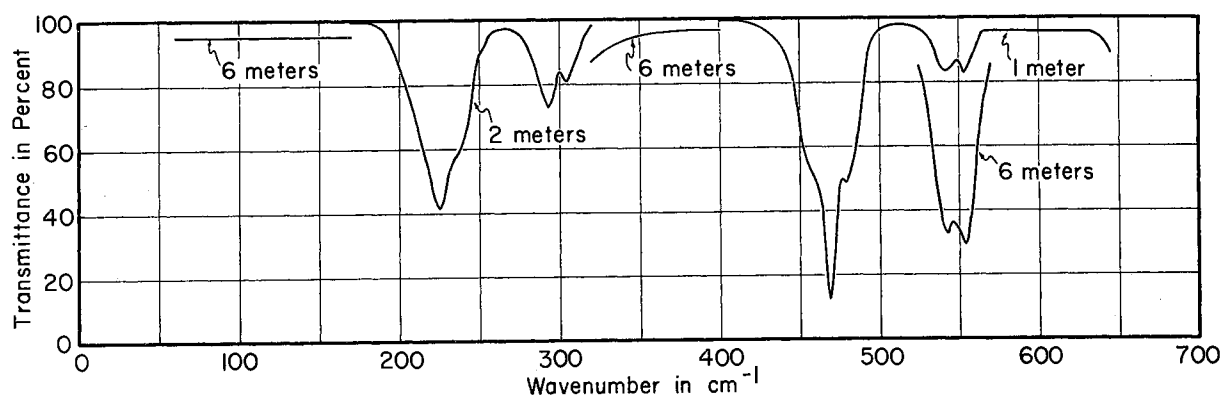
Spectra

The far infrared spectra of eighteen compounds in both liquid and vapor states are presented in the following pages. The experimental conditions and the source and purity of the compound are indicated in each figure. Following each figure is a table which lists the positions of the absorption maxima in the spectra. All values in the tables are wavenumbers in cm^{-1} .



COMPOUND 2-METHYL- THIOPHENE $C_5 H_6 S$	SOURCE AND PURITY API RESEARCH PROJECT 48A 99.8 MOLE %	STATE: SOLUTION TEMPERATURE: ROOM CELL LENGTH: AS INDICATED	SOLVENT: CYCLOPENTANE OR 2,2,4-TRIMETHYLPENTANE CONCENTRATION: AS INDICATED INSTRUMENT P-E 301
--	--	---	---

LABORATORY
 BUREAU OF MINES
 PETROLEUM RES. CTR.
 BARTLESVILLE, OKLA.



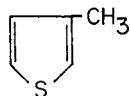
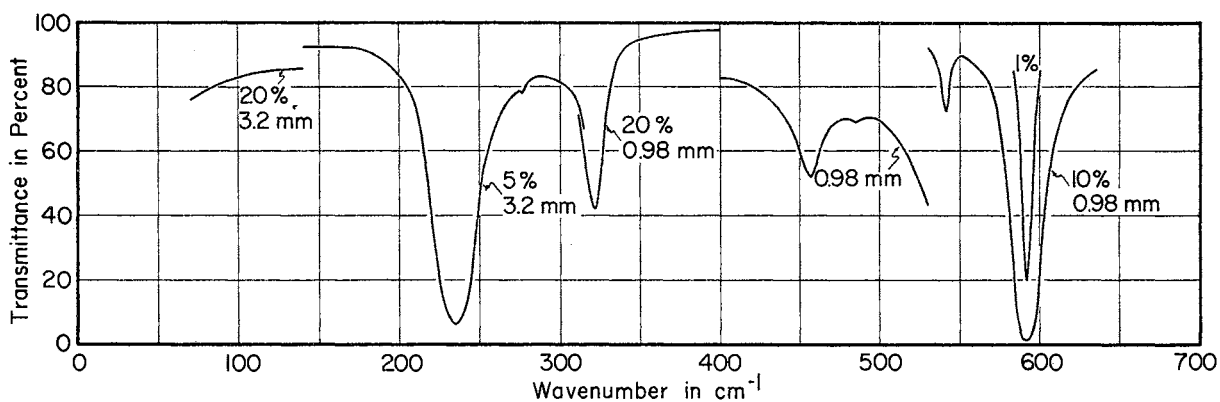
COMPOUND 2-METHYL- THIOPHENE $C_5 H_6 S$	SOURCE AND PURITY API RESEARCH PROJECT 48A 99.8 MOLE %	STATE: VAPOR TEMPERATURE: ROOM CELL LENGTH: AS INDICATED	PRESSURE: 22 mm Hg INSTRUMENT: P-E 301
--	--	--	---

LABORATORY
 BUREAU OF MINES
 PETROLEUM RES. CTR.
 BARTLESVILLE, OKLA.

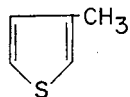
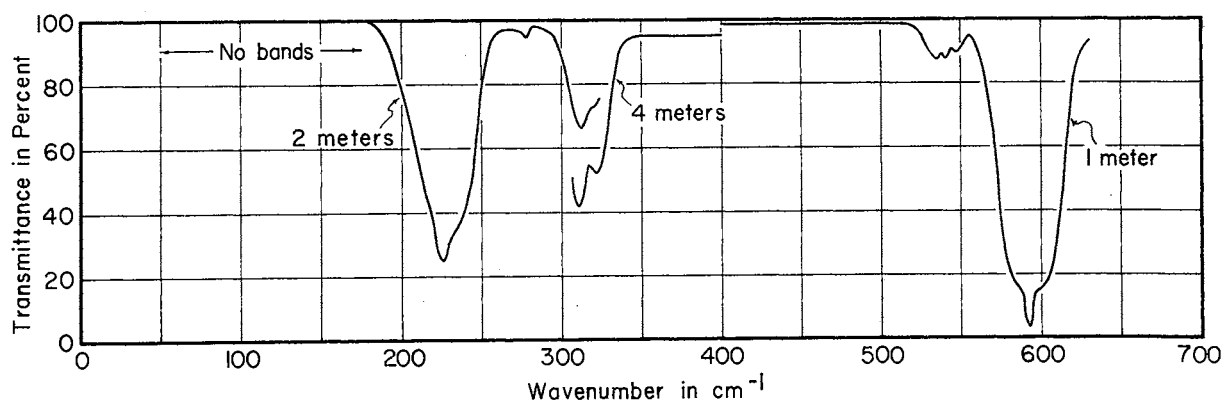
Figure 1 — Spectra of 2-Methylthiophene.

TABLE I
FAR INFRARED ABSORPTION MAXIMA FOR 2-METHYLTHIOPHENE

Liquid or Solution	Vapor
195 sh.	
234	{ 215 P sh. 225 Q 235 R. sh.
302	{ 293 P 304 R
469	{ 460 P 469 Q 479 R
547	{ 543 P 554 R



COMPOUND 3-METHYL- THIOPHENE C_5H_6S	SOURCE AND PURITY API RESEARCH PROJECT 48A 99.8 MOLE %	STATE: LIQUID OR SOLUTION TEMPERATURE: ROOM CELL LENGTH: AS INDICATED	SOLVENT: CYCLOPENTANE OR 2,2,4-TRIMETHYLPENTANE CONCENTRATION: AS INDICATED INSTRUMENT P-E 301
LABORATORY BUREAU OF MINES PETROLEUM RES. CTR. BARTLESVILLE, OKLA.			

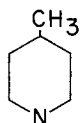
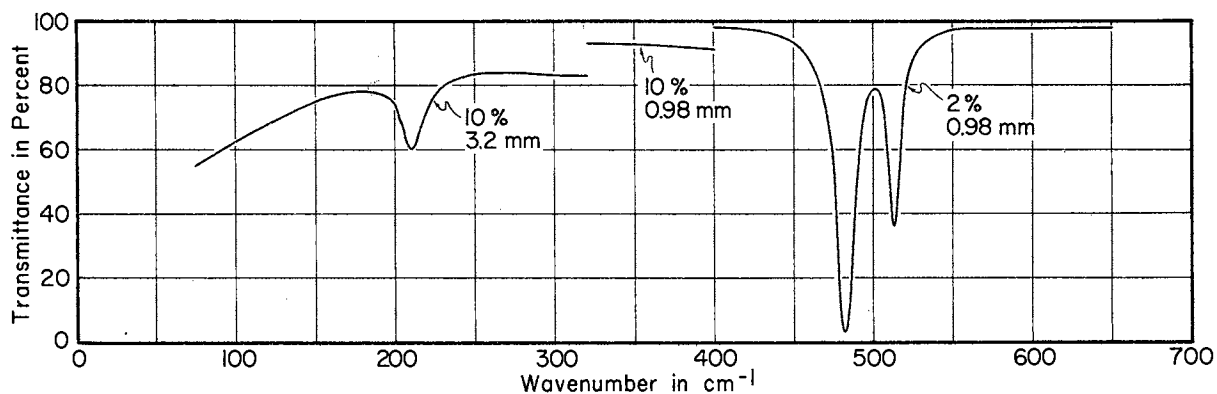


COMPOUND 3-METHYL- THIOPHENE C_5H_6S	SOURCE AND PURITY API RESEARCH PROJECT 48A 99.8 MOLE %	STATE: VAPOR TEMPERATURE: ROOM CELL LENGTH: AS INDICATED	PRESSURE: 20 mm Hg INSTRUMENT: P-E 301
LABORATORY BUREAU OF MINES PETROLEUM RES. CTR. BARTLESVILLE, OKLA.			

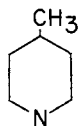
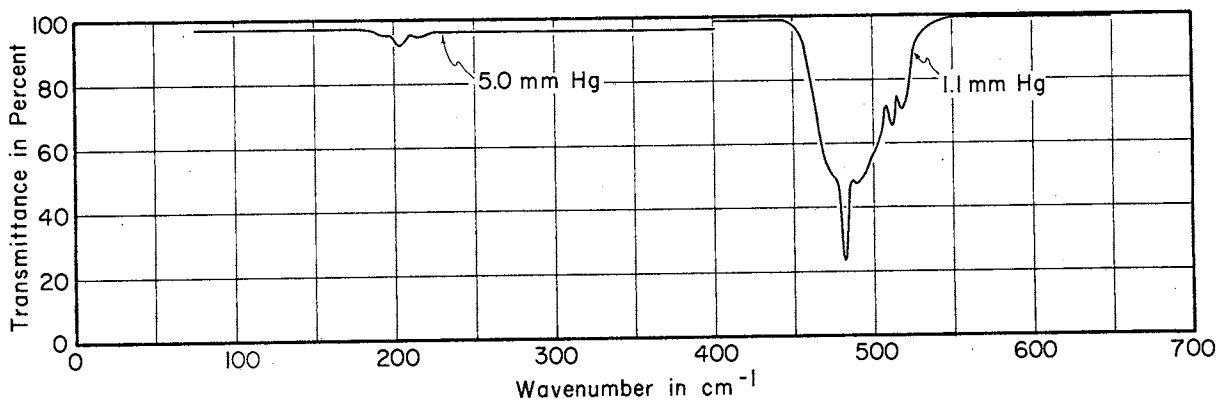
Figure 2 — Spectra of 3-Methylthiophene.

TABLE II
FAR INFRARED ABSORPTION MAXIMA FOR 3-METHYLTHIOPHENE

Liquid or Solution	Vapor
235	{ 217 P sh. 226 Q 235 R sh.
276	278
322	{ 311 P 322 R
457	
485	
542	{ 535 P 540 Q 547 R
592	{ 585 P 593 Q 600 R



COMPOUND 4-METHYL- PYRIDINE (γ -picoline) C_6H_7N	SOURCE AND PURITY API RESEARCH PROJECT 48A 9997 \pm 001 MOLE %	STATE: SOLUTION TEMPERATURE: ROOM CELL LENGTH: AS INDICATED	SOLVENT: CYCLOPENTANE OR 2,2,4-TRIMETHYLPENTANE CONCENTRATION: AS INDICATED INSTRUMENT P-E 301
LABORATORY BUREAU OF MINES PETROLEUM RES. CTR. BARTLESVILLE, OKLA.			



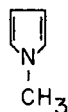
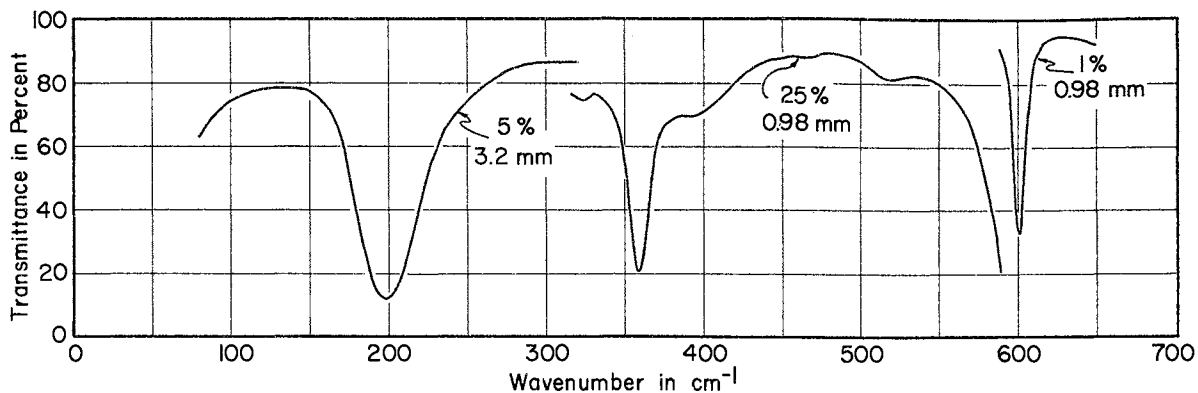
COMPOUND 4-METHYL- PYRIDINE (γ -picoline) C_6H_7N	SOURCE AND PURITY API RESEARCH PROJECT 48A 9997 \pm 001 MOLE %	STATE: VAPOR TEMPERATURE: ROOM CELL LENGTH: 6 METERS	PRESSURE: AS INDICATED INSTRUMENT: P-E 301
LABORATORY BUREAU OF MINES PETROLEUM RES. CTR. BARTLESVILLE, OKLA.			

Figure 3 — Spectra of 4-Methylpyridine.

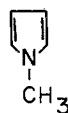
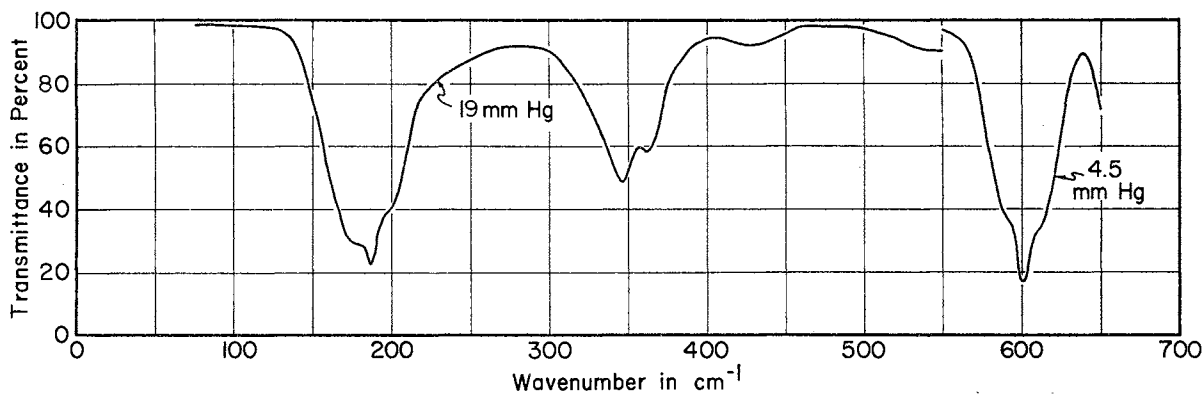
TABLE III

FAR INFRARED ABSORPTION MAXIMA FOR 4-METHYLPYRIDINE

Liquid or Solution	Vapor
210	{ 195 P 203 Q 215 R
482	{ 475 P sh. 482 Q 489 R
513	{ P 512 Q 518 R



COMPOUND 1-METHYL- PYRROLE C ₅ H ₇ N	SOURCE AND PURITY API RESEARCH PROJECT 52 99.998 ± 0.001 MOLE %	STATE: SOLUTION TEMPERATURE: ROOM CELL LENGTH: AS INDICATED	SOLVENT: CYCLOPENTANE OR 2,2,4-TRIMETHYLPENTANE CONCENTRATION: AS INDICATED INSTRUMENT: P-E 301
LABORATORY BUREAU OF MINES PETROLEUM RES. CTR. BARTLESVILLE, OKLA.			

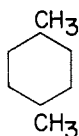
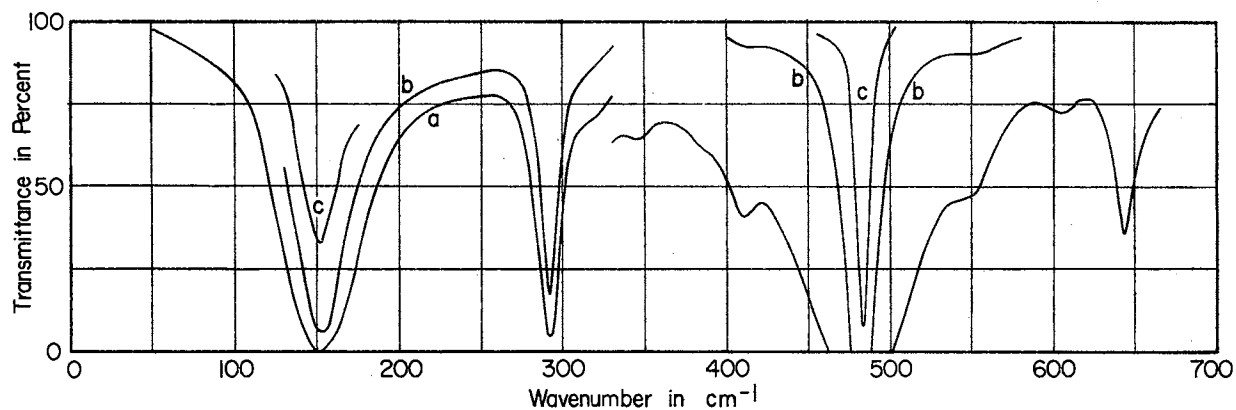


COMPOUND 1-METHYL- PYRROLE C ₅ H ₇ N	SOURCE AND PURITY API RESEARCH PROJECT 52 99.998 ± 0.001 MOLE %	STATE: VAPOR TEMPERATURE: ROOM CELL LENGTH: 3 METERS	PRESSURE: AS INDICATED INSTRUMENT: P-E 301
LABORATORY BUREAU OF MINES PETROLEUM RES. CTR. BARTLESVILLE, OKLA.			

Figure 4 — Spectra of 1-Methylpyrrole.

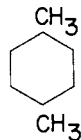
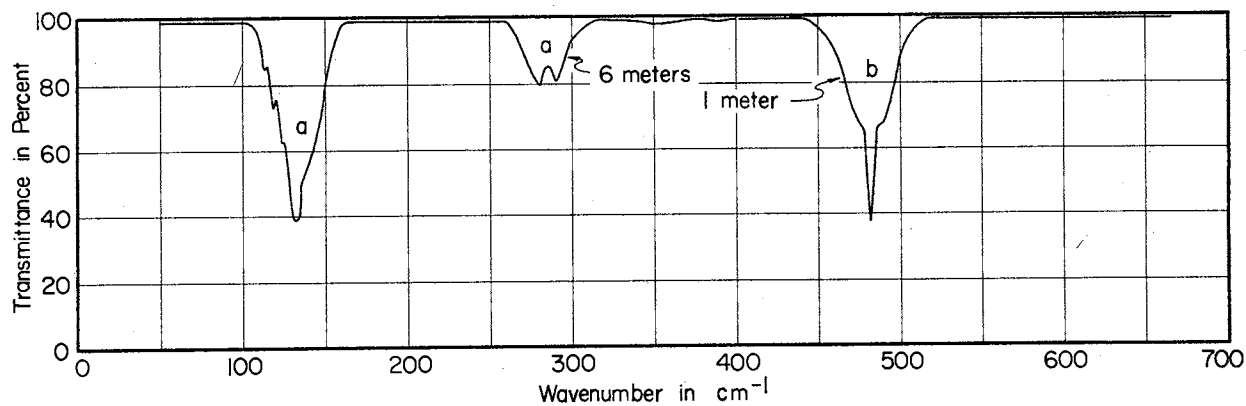
TABLE IV
FAR INFRARED ABSORPTION MAXIMA FOR 1-METHYLPYRROLE

Liquid or Solution	Vapor
198	{ 178 P sh. 186 Q 198 R.sh.
324	
359	{ 346 P 361 R
393	
519	425
602	{ P 601 Q R



COMPOUND 1,4-DIMETHYLBENZENE (p-Xylene) C ₈ H ₁₀	SOURCE & PURITY PHILLIPS PETROLEUM CO. RESEARCH GRADE	STATE: LIQUID OR SOLUTION TEMPERATURE: ROOM CELL LENGTH: 32 mm below 330 cm ⁻¹ , 0.98 mm above	a, 25%; b, 10%; c, 1% SOLVENT: BENZENE, CS ₂ , & 2,2,4-TRIMETHYLPENTANE INSTRUMENT: P-E 301
---	--	--	--

LABORATORY
BUREAU OF MINES
PETROLEUM RES. CTR.
BARTLESVILLE, OKLA.



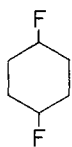
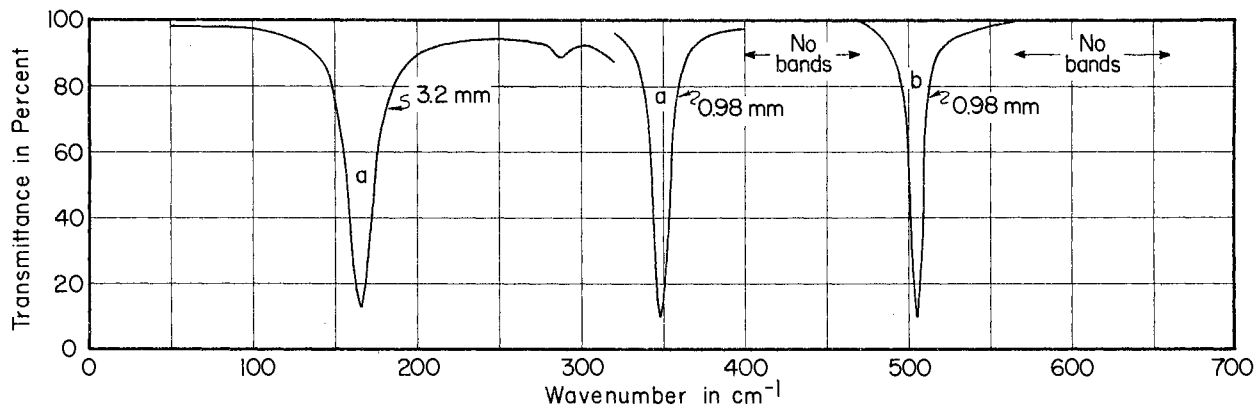
COMPOUND 1,4-DIMETHYLBENZENE (para-Xylene) C ₈ H ₁₀	SOURCE & PURITY PHILLIPS PETROLEUM CO. RESEARCH GRADE	STATE: VAPOR TEMPERATURE: ROOM CELL LENGTH AS INDICATED	PRESSURE: a, ABOUT 8 mm Hg b, ABOUT 2 mm Hg INSTRUMENT: P-E 301
--	--	--	--

LABORATORY
BUREAU OF MINES
PETROLEUM RES. CTR.
BARTLESVILLE, OKLA.

Figure 5 — Spectra of 1,4-Dimethylbenzene.

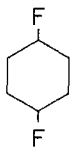
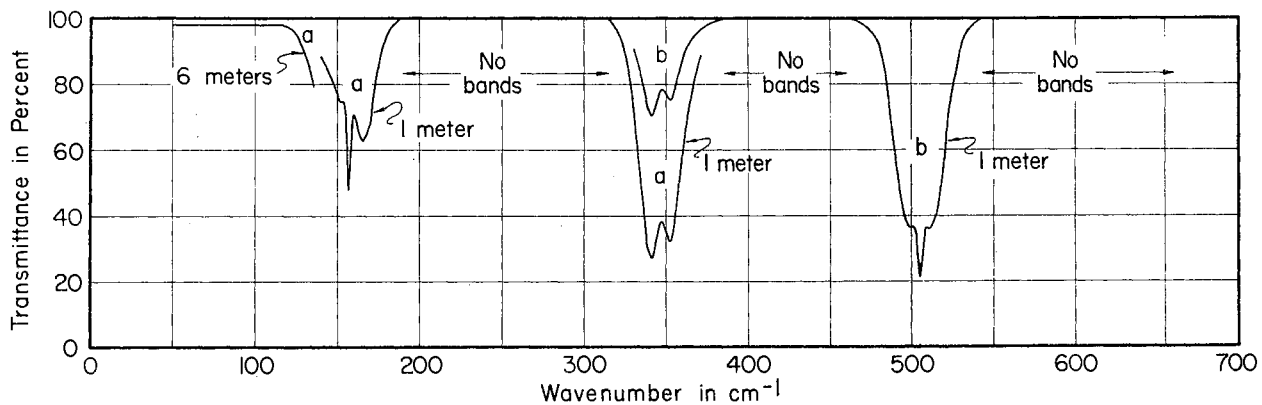
TABLE V
 FAR INFRARED ABSORPTION MAXIMA FOR 1,4-DIMETHYLBENZENE

Liquid or Solution	Vapor
152	{ P 132 Q R
292	{ 280 P 290 R
345	350
385 sh.	389
410	
484	{ 475 P sh. 481 Q 487 R sh.
550 sh.	
605	
644	



COMPOUND 1,4-DIFLUORO- BENZENE $C_6H_4F_2$	SOURCE AND PURITY PURIFIED FROM DONATED SAMPLE	STATE: SOLUTION TEMPERATURE: ROOM CELL LENGTH: AS INDICATED	SOLVENT: CYCLOPENTANE OR 2,2,4-TRIMETHYLPENTANE CONCENTRATION: a, 5%; b, 1% INSTRUMENT: P-E 301
---	--	--	---

LABORATORY
BUREAU OF MINES
PETROLEUM RES. CTR.
BARTLESVILLE, OKLA.



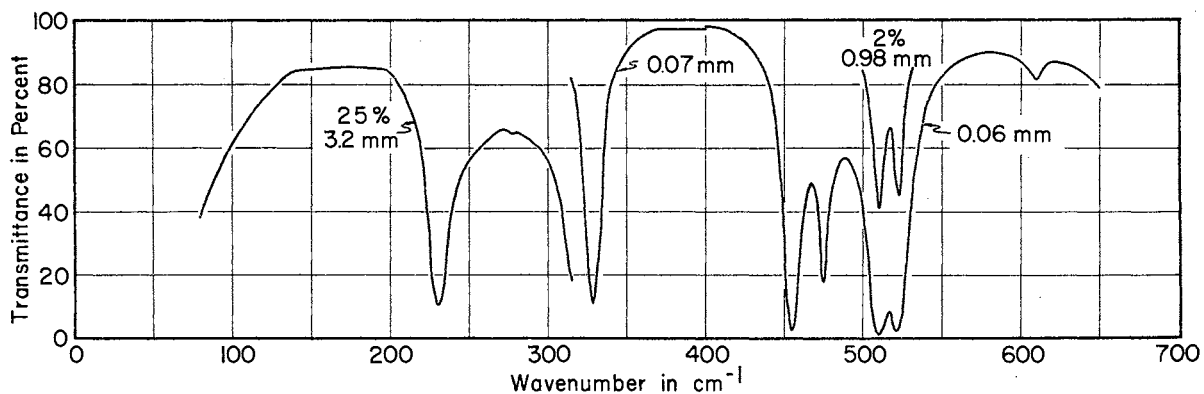
COMPOUND 1,4-DIFLUORO- BENZENE $C_6H_4F_2$	SOURCE AND PURITY PURIFIED FROM DONATED SAMPLE	STATE: VAPOR TEMPERATURE: ROOM CELL LENGTH: AS INDICATED	PRESSURE: a, 17 mm Hg b, NOT MEASURED INSTRUMENT: P-E 301
---	--	---	---

LABORATORY
BUREAU OF MINES
PETROLEUM RES. CTR.
BARTLESVILLE, OKLA.

Figure 6 — Spectra of 1,4-Difluorobenzene.

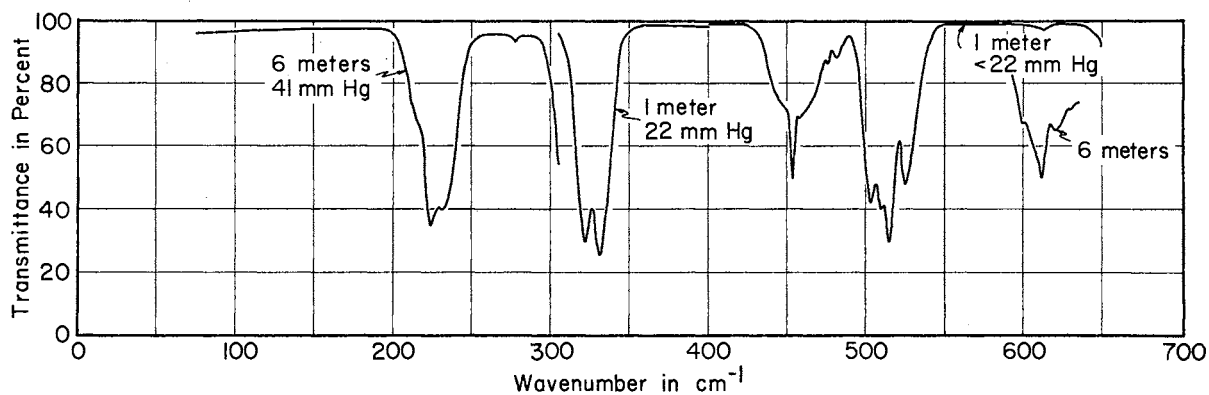
TABLE VI
FAR INFRARED ABSORPTION MAXIMA FOR 1,4-DIFLUOROBENZENE

Liquid or Solution	Vapor
166	{ 152 P 157 Q 165 R
287	
348	{ 341 P 353 R
505	{ 499 P 505 Q 511 R



COMPOUND 1,3-DIFLUORO- BENZENE $C_6H_4F_2$	SOURCE AND PURITY PURIFIED FROM ILL. STATE GEOL. SURVEY DIV. SAMPLE 99.999 ± 0.001 MOLE %	STATE: LIQUID OR SOLUTION TEMPERATURE: ROOM CELL LENGTH: AS INDICATED	SOLVENT: CYCLOPENTANE OR 2,2,4-TRIMETHYLPENTANE CONCENTRATION: AS INDICATED INSTRUMENT: P-E 301
---	---	---	---

LABORATORY
BUREAU OF MINES
PETROLEUM RES. CTR.
BARTLESVILLE, OKLA.



COMPOUND 1,3-DIFLUORO- BENZENE $C_6H_4F_2$	SOURCE AND PURITY PURIFIED FROM ILL. STATE GEOL. SURVEY DIV. SAMPLE 99.999 ± 0.001 MOLE %	STATE: VAPOR TEMPERATURE: ROOM CELL LENGTH: AS INDICATED	PRESSURE: AS INDICATED OR UNKNOWN INSTRUMENT: P-E 301
---	---	---	---

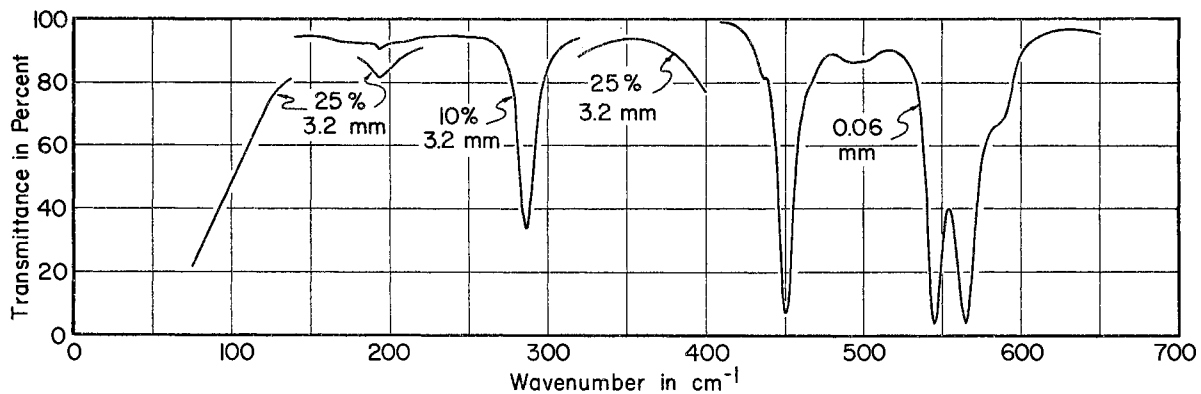
LABORATORY
BUREAU OF MINES
PETROLEUM RES. CTR.
BARTLESVILLE, OKLA.

Figure 7 — Spectra of 1,3-Difluorobenzene.

TABLE VII

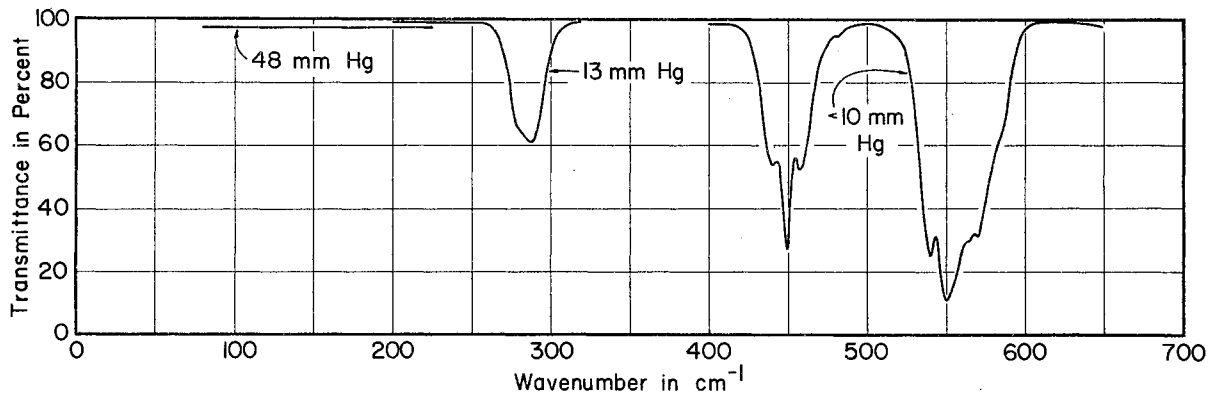
FAR INFRARED ABSORPTION MAXIMA FOR 1,3-DIFLUOROBENZENE

Liquid or Solution	Vapor
230	{ P 224 Q 231 R
277	277
329	{ 322 P 331 R
455	{ P 454 Q 458 R
475	{ P 476 Q 482 R
510	{ 503 P 510 Q R
523	{ 515 P 525 R
610	{ 599 P 612 Q 620 R



COMPOUND 1,2-DIFLUORO- BENZENE $C_6H_4F_2$	SOURCE AND PURITY PURIFIED FROM ILL. STATE GEOL. SURVEY DIV. SAMPLE 99.998 ± 0.002 MOLE %	STATE: LIQUID OR SOLUTION TEMPERATURE: ROOM CELL LENGTH: AS INDICATED	SOLVENT: CYCLOPENTANE CONCENTRATION: AS INDICATED INSTRUMENT: P-E 301
---	---	---	--

LABORATORY
BUREAU OF MINES
PETROLEUM RES. CTR.
BARTLESVILLE, OKLA.



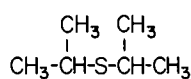
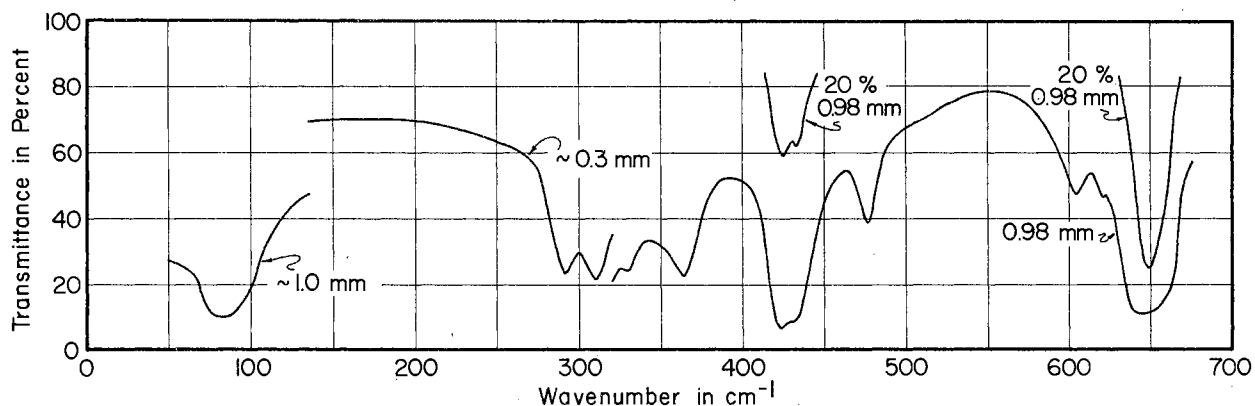
COMPOUND 1,2-DIFLUORO- BENZENE $C_6H_4F_2$	SOURCE AND PURITY PURIFIED FROM ILL. STATE GEOL. SURVEY DIV. SAMPLE 99.998 ± 0.002 MOLE %	STATE: VAPOR TEMPERATURE: ROOM CELL LENGTH: 6 METERS	PRESSURE: AS INDICATED INSTRUMENT: P-E 301
---	---	---	--

LABORATORY
BUREAU OF MINES
PETROLEUM RES. CTR.
BARTLESVILLE, OKLA.

Figure 8 — Spectra of 1,2-Difluorobenzene.

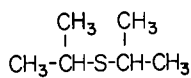
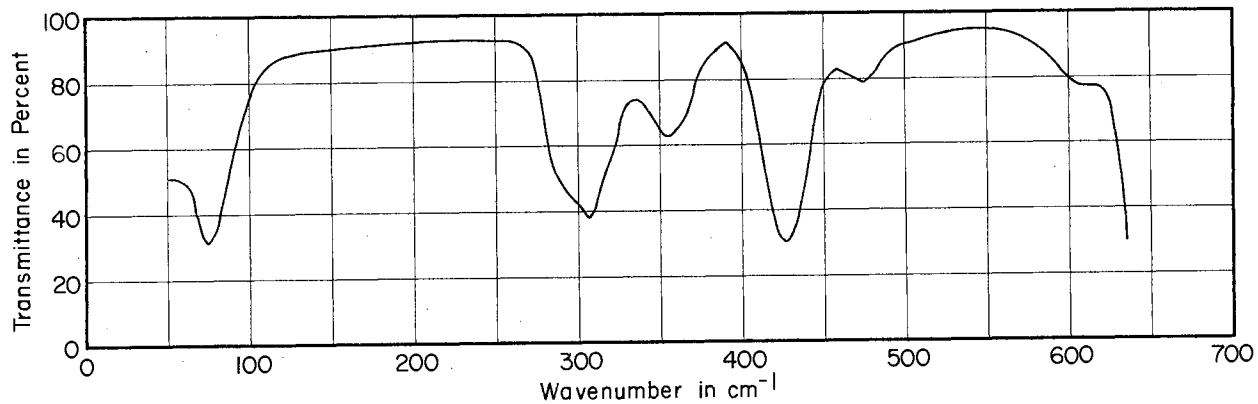
TABLE VIII
FAR INFRARED ABSORPTION MAXIMA FOR 1,2-DIFLUOROBENZENE

Liquid or Solution	Vapor
193	
286	287
437	
451	{ 441 P 450 Q 458 R
495	
545	{ 541 P 551 R
565	{ P 565 Q 571 R
587 sh.	



COMPOUND 2,4-DIMETHYL-3- THIAPENTANE (Diisopropyl sulfide) $\text{C}_6\text{H}_{14}\text{S}$	SOURCE AND PURITY API RESEARCH PROJECT 48 99.99 ± 0.01 MOLE %	STATE: LIQUID OR SOLUTION TEMPERATURE: ROOM CELL LENGTH: AS INDICATED	SOLVENT: CYCLOPENTANE OR 2,2,4-TRIMETHYLPENTANE CONCENTRATION: AS INDICATED INSTRUMENT P-E 301
---	---	--	---

LABORATORY
 BUREAU OF MINES
 PETROLEUM RES. CTR.
 BARTLESVILLE, OKLA.



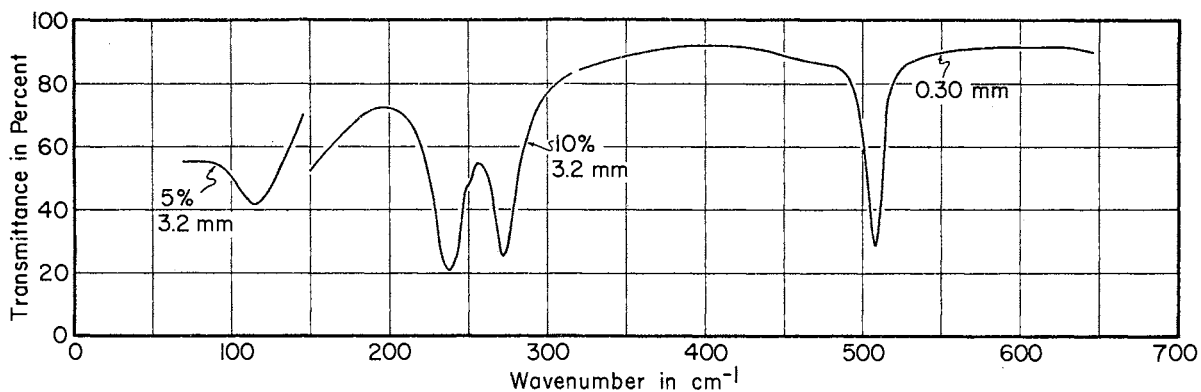
COMPOUND 2,4-DIMETHYL-3- THIAPENTANE (Diisopropyl sulfide) $\text{C}_6\text{H}_{14}\text{S}$	SOURCE AND PURITY API RESEARCH PROJECT 48 99.99 ± 0.01 MOLE %	STATE: VAPOR TEMPERATURE: ROOM CELL LENGTH: 6 METERS	PRESSURE: 17 mm Hg INSTRUMENT P-E 301
---	---	---	--

LABORATORY
 BUREAU OF MINES
 PETROLEUM RES. CTR.
 BARTLESVILLE, OKLA.

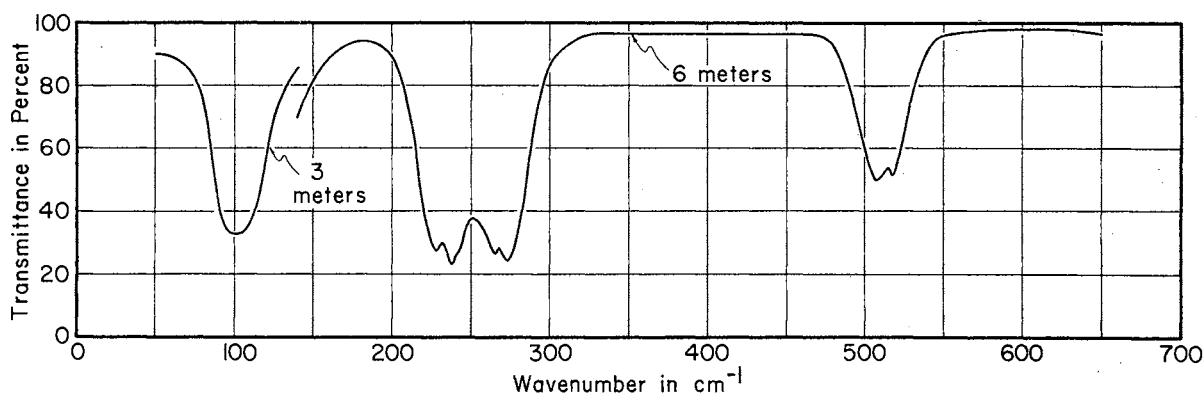
Figure 9 — Spectra of 2,4-Dimethyl-3-thiapentane.

TABLE IX
FAR INFRARED ABSORPTION MAXIMA FOR
2,4-DIMETHYL-3-THIAPENTANE

Liquid or Solution	Vapor
83	74
291	290 sh.
310	306
330	
363	354
424	426
432	
476	474
604	
620	610
648	



$\text{CH}_3\text{-S-S-CH}_3$ COMPOUND 2,3-DITHIA- BUTANE (Dimethyl- disulfide) $\text{C}_2\text{H}_6\text{S}_2$	SOURCE AND PURITY API RESEARCH PROJECT 48A 99.97 ± 0.02 MOLE %	STATE: LIQUID OR SOLUTION TEMPERATURE: ROOM CELL LENGTH: AS INDICATED	SOLVENT: CYCLOPENTANE OR 2,2,4-TRIMETHYLPENTANE
			CONCENTRATION: AS INDICATED INSTRUMENT: P-E 301
			LABORATORY BUREAU OF MINES PETROLEUM RES. CTR. BARTLESVILLE, OKLA.

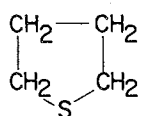
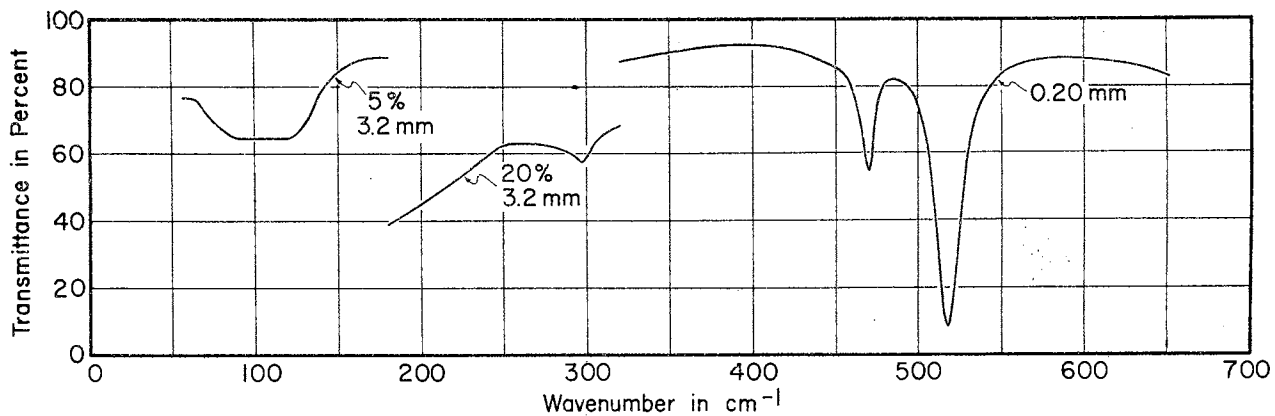


$\text{CH}_3\text{-S-S-CH}_3$ COMPOUND 2,3-DITHIA- BUTANE (Dimethyl- disulfide) $\text{C}_2\text{H}_6\text{S}_2$	SOURCE AND PURITY API RESEARCH PROJECT 48A 99.97 ± 0.02 MOLE %	STATE: VAPOR TEMPERATURE: ROOM CELL LENGTH: AS INDICATED	PRESSURE: 26 mm Hg
			INSTRUMENT: P-E 301
			LABORATORY BUREAU OF MINES PETROLEUM RES. CTR. BARTLESVILLE, OKLA.

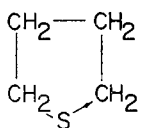
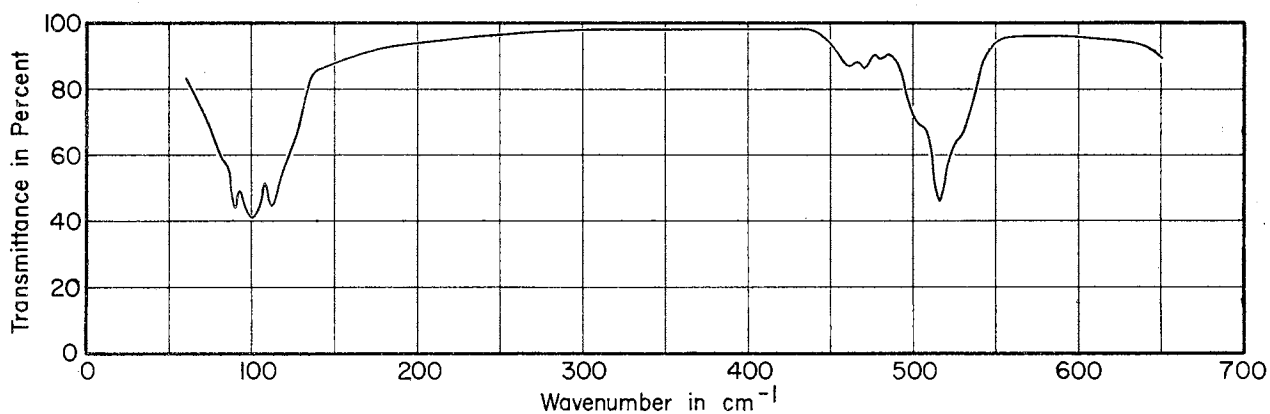
Figure 10 — Spectra of 2,3-Dithiabutane.

TABLE X
FAR INFRARED ABSORPTION MAXIMA FOR 2,3-DITHIABUTANE

Liquid or Solution	Vapor
115	101
238	{ 228 P 238 Q R
250 sh.	
272	{ 266 P 273 Q R
508	{ P 508 Q 518 R



COMPOUND THIACYCLO- PENTANE $\text{C}_4\text{H}_8\text{S}$	SOURCE AND PURITY API RESEARCH PROJECT 48A 99.987 ± 0.005 MOLE %	STATE: LIQUID OR SOLUTION TEMPERATURE: ROOM CELL LENGTH: AS INDICATED	SOLVENT: CYCLOPENTANE CONCENTRATION: AS INDICATED INSTRUMENT: P-E 301
LABORATORY BUREAU OF MINES PETROLEUM RES. CTR. BARTLESVILLE, OKLA.			

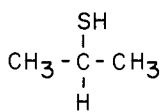
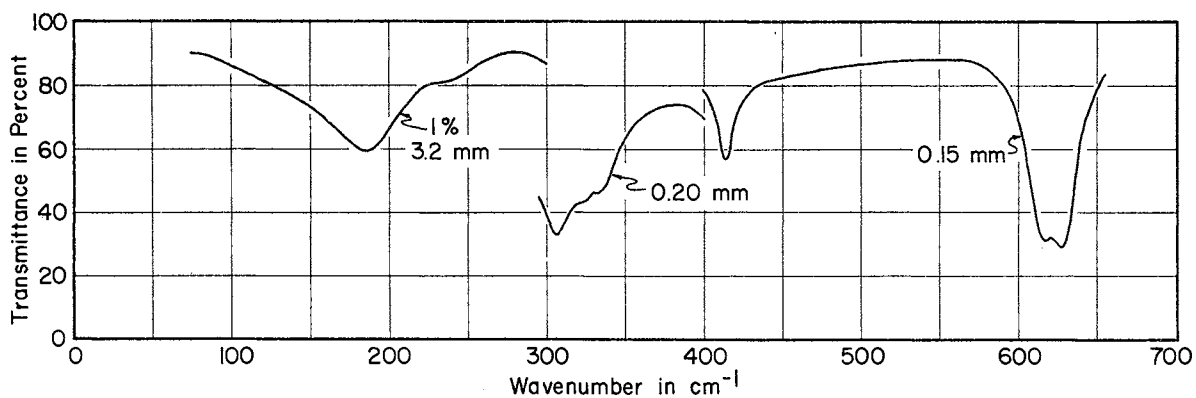


COMPOUND THIACYCLO- PENTANE $\text{C}_4\text{H}_8\text{S}$	SOURCE AND PURITY API RESEARCH PROJECT 48A 99.987 ± 0.005 MOLE %	STATE: VAPOR TEMPERATURE: ROOM CELL LENGTH: 6 METERS	PRESSURE: 17 mm Hg INSTRUMENT: P-E 301
LABORATORY BUREAU OF MINES PETROLEUM RES. CTR. BARTLESVILLE, OKLA.			

Figure 11 — Spectra of Thiacyclopentane.

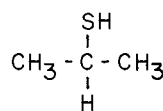
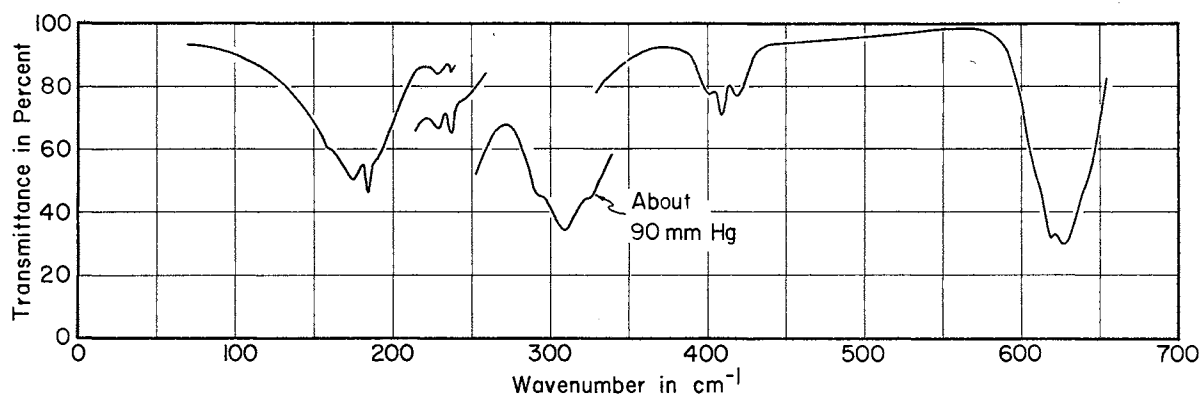
TABLE XI
FAR INFRARED ABSORPTION MAXIMA FOR THIACYCLOPENTANE

Liquid or Solution	Vapor
105	{ 90 P 100 Q 112 R
297	
470	{ 461 P 470 Q 480 R
518	{ 505 P sh. 516 Q 527 R sh.



COMPOUND 2-PROPANETHIOL (Isopropyl mercaptan) $\text{C}_3\text{H}_8\text{S}$	SOURCE AND PURITY API RESEARCH PROJECT 48 99.98 ± 0.02 MOLE %	STATE: LIQUID OR SOLUTION TEMPERATURE: ROOM CELL LENGTH: AS INDICATED	SOLVENT: CYCLOPENTANE CONCENTRATION: AS INDICATED INSTRUMENT: P-E 301
--	--	---	--

LABORATORY
BUREAU OF MINES
PETROLEUM RES. CTR.
BARTLESVILLE, OKLA.



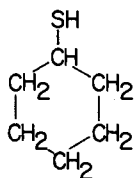
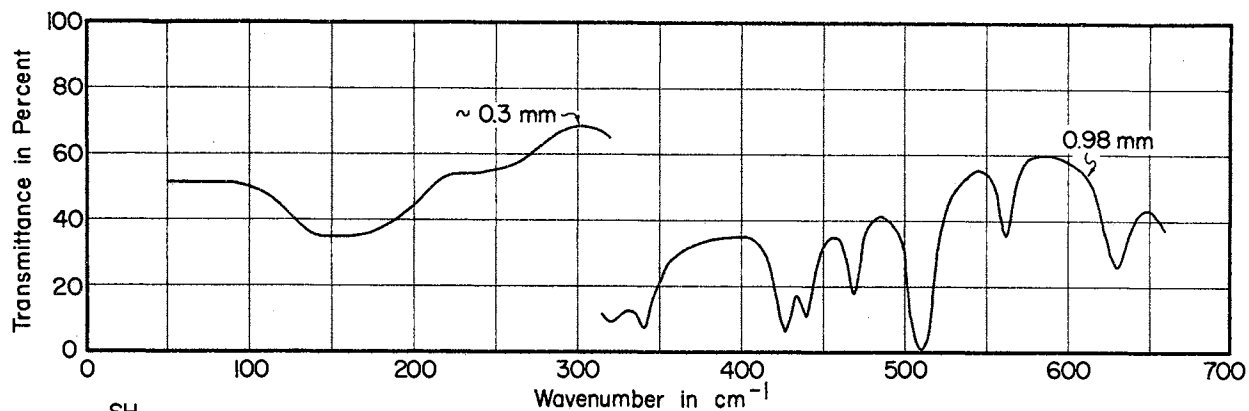
COMPOUND 2-PROPANETHIOL (Isopropyl mercaptan) $\text{C}_3\text{H}_8\text{S}$	SOURCE AND PURITY API RESEARCH PROJECT 48 99.98 ± 0.02 MOLE %	STATE: VAPOR TEMPERATURE: ROOM CELL LENGTH: 1 METER	PRESSURE: AS INDICATED OR UNKNOWN INSTRUMENT: P-E 301
--	--	--	---

LABORATORY
BUREAU OF MINES
PETROLEUM RES. CTR.
BARTLESVILLE, OKLA.

Figure 12 — Spectra of 2-Propanethiol.

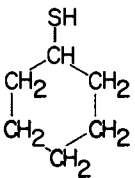
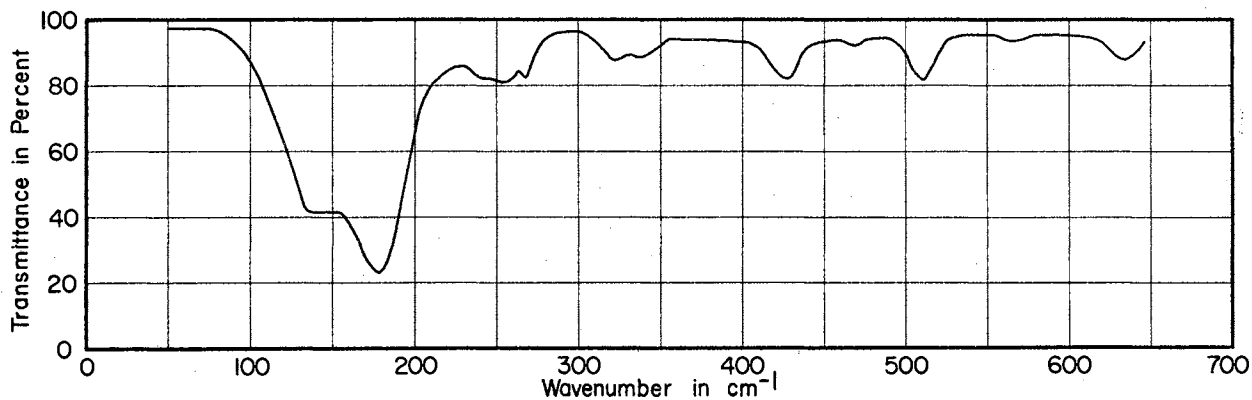
TABLE XII
FAR INFRARED ABSORPTION MAXIMA FOR 2-PROPANETHIOL

Liquid or Solution	Vapor
	160 sh.
186	{ 175 P 185 Q R
235 sh.	{ 230 P 238 Q 245 R
	295 sh.
306	310
322	325 sh.
332	
414	{ 402 P 410 Q 420 R
617	620
628	628



COMPOUND CYCLOHEXANE- THIOL (Cyclohexyl mercaptan) $C_6H_{12}S$	SOURCE AND PURITY API RESEARCH PROJECT 48 9995 ± 0.05 MOLE %	STATE: LIQUID	INSTRUMENT P-E 301
		TEMPERATURE: ROOM CELL LENGTH: AS INDICATED	

LABORATORY
BUREAU OF MINES
PETROLEUM RES. CTR.
BARTLESVILLE, OKLA.



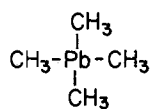
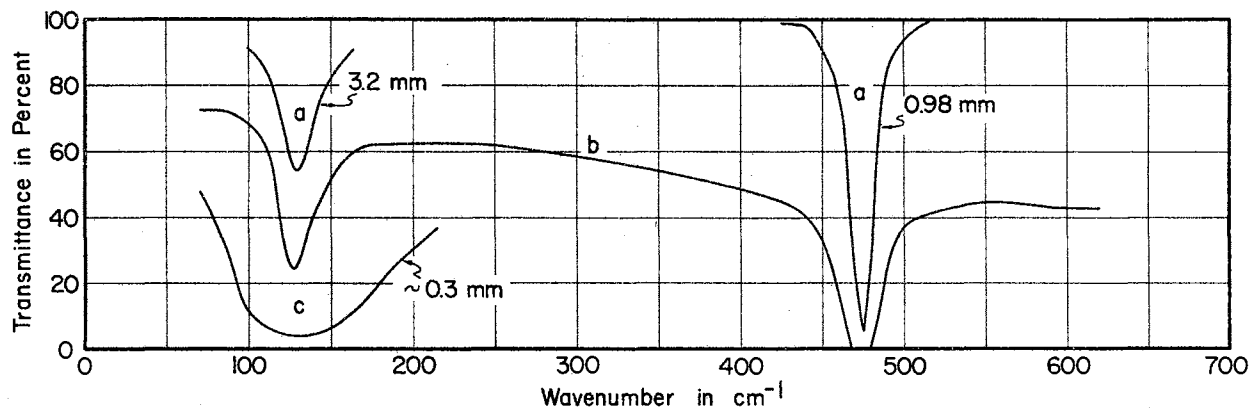
COMPOUND CYCLOHEXANE- THIOL (Cyclohexyl mercaptan) $C_6H_{12}S$	SOURCE AND PURITY API RESEARCH PROJECT 48 9995 ± 0.05 MOLE %	STATE: VAPOR	PRESSURE: 4 mm Hg
		TEMPERATURE: ROOM CELL LENGTH: 6 METERS	INSTRUMENT P-E 301

LABORATORY
BUREAU OF MINES
PETROLEUM RES. CTR.
BARTLESVILLE, OKLA.

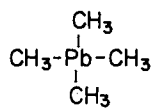
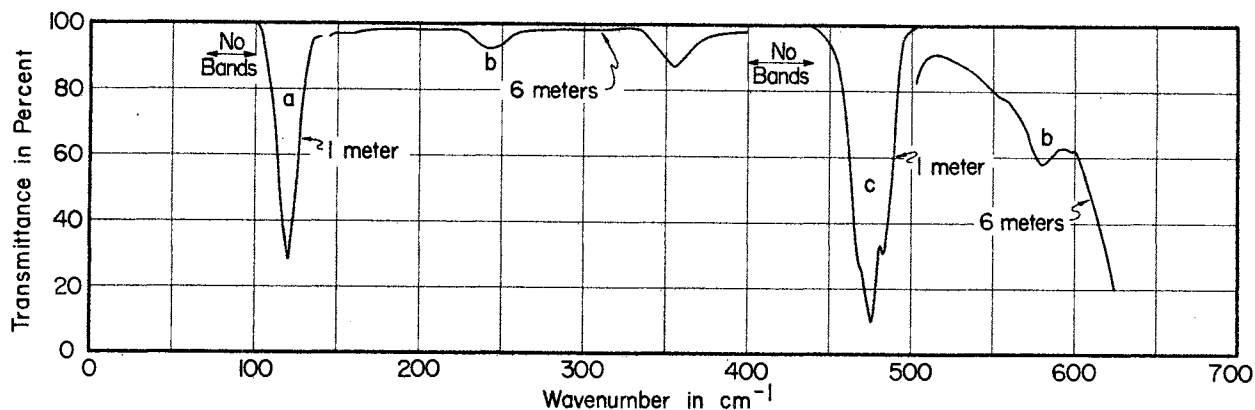
Figure 13 — Spectra of Cyclohexanethiol.

TABLE XIII
FAR INFRARED ABSORPTION MAXIMA FOR CYCLOHEXANETHIOL

Liquid or Solution	Vapor
	145
140-170	178
250 sh.	{ 243 P 255 Q 267 R
320	322
330	336
427	428
440	
469	469
510	510
562	565
630	634



COMPOUND TETRA- METHYLLEAD $\text{C}_4 \text{H}_{12} \text{Pb}$	SOURCE AND PURITY ETHYL CORP. ABOUT 99.95 MOLE %	STATE: a, SOLUTION b, ABSORBED IN POLY- ETHYLENE c, LIQUID TEMPERATURE: ROOM CELL LENGTH: AS INDICATED	SOLVENT: CYCLOPENTANE CONCENTRATION: $\frac{1}{2}$ % INSTRUMENT P-E 301
			LABORATORY BUREAU OF MINES PETROLEUM RES. CTR. BARTLESVILLE, OKLA.

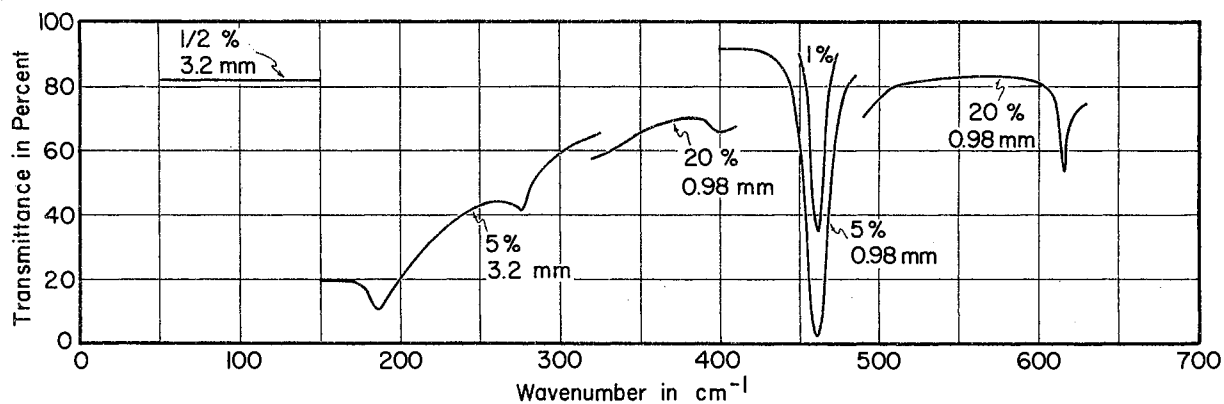


COMPOUND TETRA- METHYLLEAD $\text{C}_4 \text{H}_{12} \text{Pb}$	SOURCE AND PURITY ETHYL CORP. ABOUT 99.95 MOLE %	STATE: VAPOR TEMPERATURE: ROOM CELL LENGTH: AS INDICATED	PRESSURE: a & c, NOT MEASURED, <1mm Hg b, 7 mm Hg INSTRUMENT P-E 301
			LABORATORY BUREAU OF MINES PETROLEUM RES. CTR. BARTLESVILLE, OKLA.

Figure 14 — Spectra of Tetramethyllead.

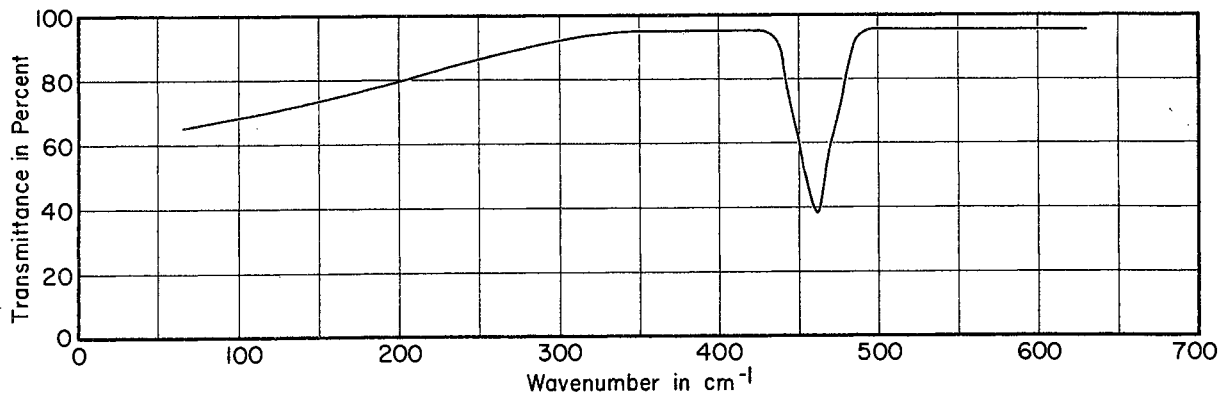
TABLE XIV
FAR INFRARED ABSORPTION MAXIMA FOR TETRAMETHYLLEAD

Liquid or Solution	Vapor
130	120
	243
	355
475	{ 463 P sh. 476 Q 483 R
	580
	599



COMPOUND BENZENE- THIOL C_6H_6S	SOURCE AND PURITY API RESEARCH PROJECT 48A 99.9 MOLE %	STATE: SOLUTION TEMPERATURE: ROOM CELL LENGTH: AS INDICATED	SOLVENT: CYCLOPENTANE OR 2,2,4-TRIMETHYLPENTANE CONCENTRATION: AS INDICATED INSTRUMENT P-E 301
--	---	--	--

LABORATORY BUREAU OF MINES PETROLEUM RES. CTR. BARTLESVILLE, OKLA.



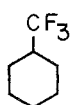
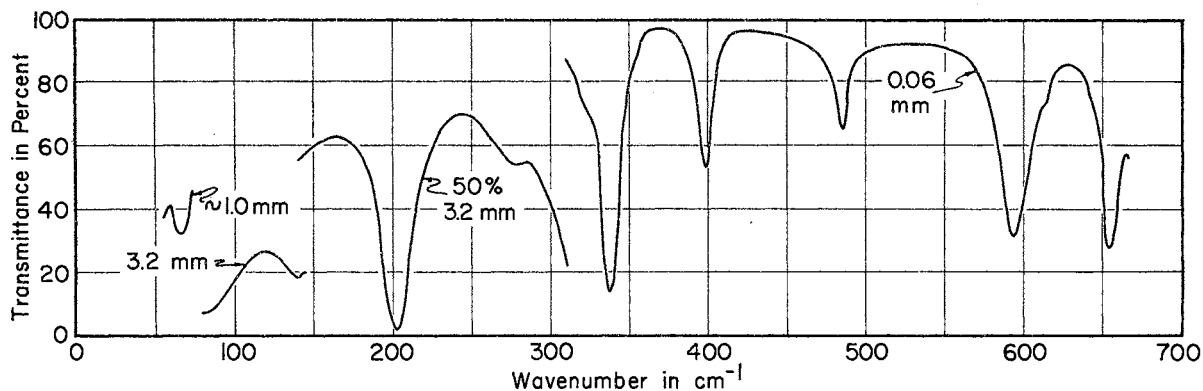
COMPOUND BENZENE- THIOL C_6H_6S	SOURCE AND PURITY API RESEARCH PROJECT 48A 99.9 MOLE %	STATE: VAPOR TEMPERATURE: ROOM CELL LENGTH: 6 METERS	PRESSURE: 1.8 mm Hg INSTRUMENT P-E 301
--	---	---	---

LABORATORY BUREAU OF MINES PETROLEUM RES. CTR. BARTLESVILLE, OKLA.

Figure 15 — Spectra of Benzenethiol.

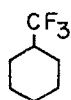
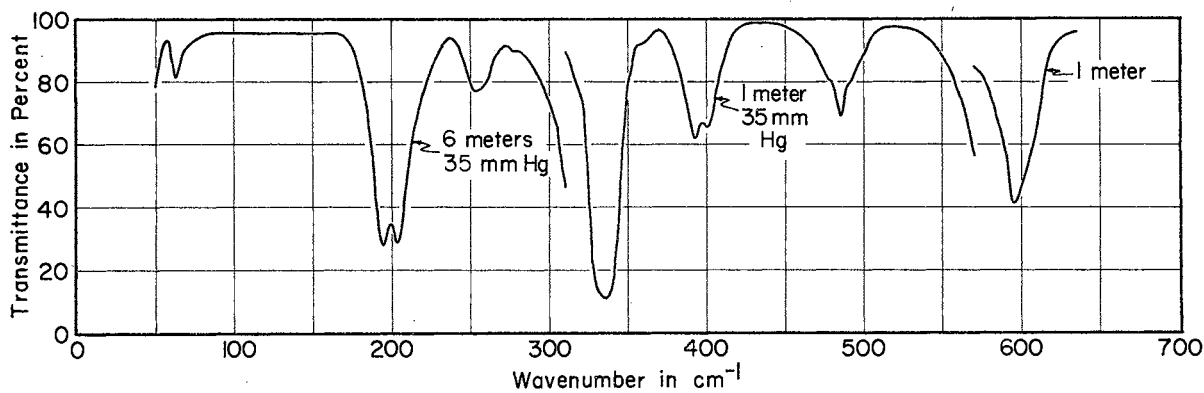
TABLE XV
FAR INFRARED ABSORPTION MAXIMA FOR BENZENETHIOL

Liquid or Solution	Vapor
186	
276	
400	
462	{ P 462 Q R
616	



COMPOUND BENZOTRI- FLUORIDE (Trifluorotoluene) $C_7H_5F_3$	SOURCE AND PURITY EASTMAN ORGANIC CHEMICALS PRACTICAL GRADE	STATE: LIQUID OR SOLUTION TEMPERATURE: ROOM CELL LENGTH: AS INDICATED	SOLVENT: CYCLOPENTANE CONCENTRATION: AS INDICATED INSTRUMENT: P-E 301
--	--	---	--

LABORATORY
BUREAU OF MINES
PETROLEUM RES. CTR.
BARTLESVILLE, OKLA.



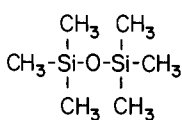
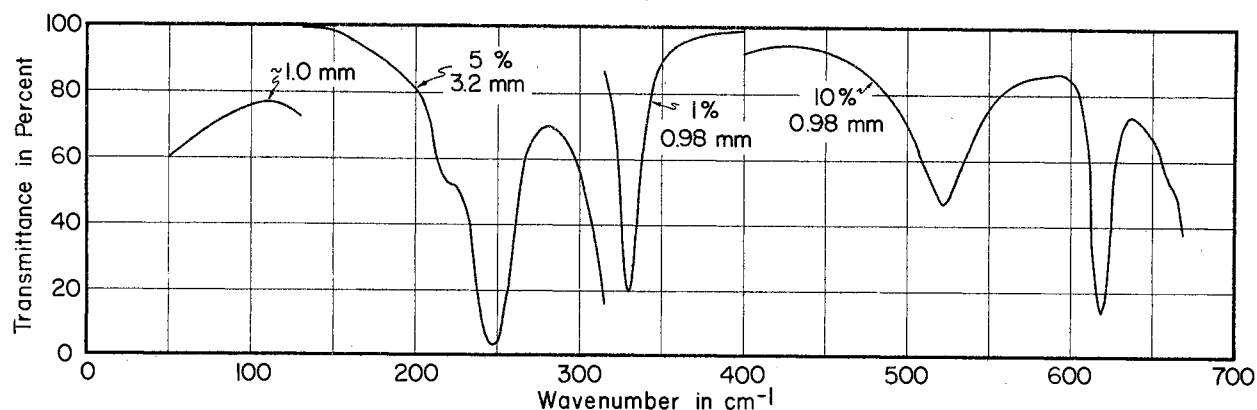
COMPOUND BENZOTRI- FLUORIDE (Trifluorotoluene) $C_7H_5F_3$	SOURCE AND PURITY EASTMAN ORGANIC CHEMICALS PRACTICAL GRADE	STATE: VAPOR TEMPERATURE: ROOM CELL LENGTH: AS INDICATED	PRESSURE: AS INDICATED INSTRUMENT: P-E 301
--	--	---	--

LABORATORY
BUREAU OF MINES
PETROLEUM RES. CTR.
BARTLESVILLE, OKLA.

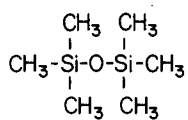
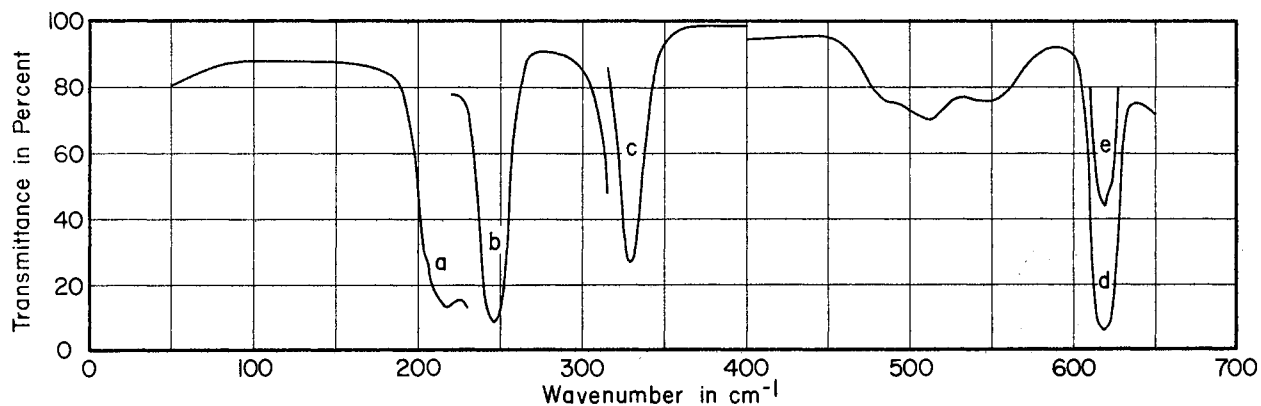
Figure 16 — Spectra of Benzotrifluoride.

TABLE XVI
 FAR INFRARED ABSORPTION MAXIMA FOR BENZOTRIFLUORIDE

Liquid or Solution	Vapor
66	63
140	
202	{ 194 P 203 R
	253
277	278
337	335
	360 sh.
398	{ 392 P 400 R
485	{ 478 P sh. 485 Q 492 R sh.
593	595
613 sh.	
654	



COMPOUND HEXAMETHYL- DISILOXANE $\text{C}_6\text{H}_{18}\text{O Si}_2$	SOURCE AND PURITY PURIFIED FROM COMMERCIAL MATERIAL 99.996 MOLE %	STATE: LIQUID OR SOLUTION TEMPERATURE: ROOM CELL LENGTH: AS INDICATED	SOLVENT: CYCLOPENTANE OR 2,2,4-TRIMETHYLPENTANE CONCENTRATION: AS INDICATED INSTRUMENT P-E 301
LABORATORY BUREAU OF MINES PETROLEUM RES. CTR. BARTLESVILLE, OKLA.			



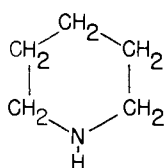
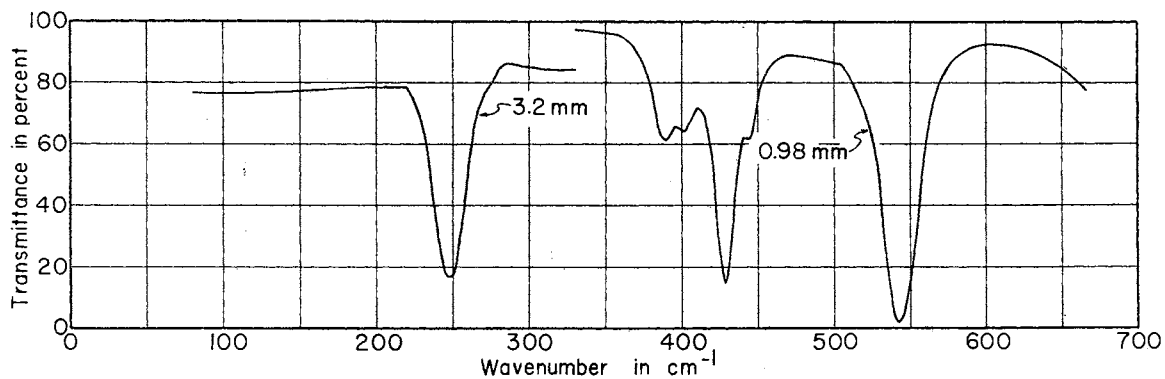
COMPOUND HEXAMETHYL- DISILOXANE $\text{C}_6\text{H}_{18}\text{O Si}_2$	SOURCE AND PURITY PURIFIED FROM COMMERCIAL MATERIAL 99.996 MOLE %	STATE: VAPOR TEMPERATURE: ROOM CELL LENGTH: a, 6 meters: b, c, d, & e, 1 meter	PRESSURE: a & d, 10 mm Hg; b, c, & e, < 10 mm Hg; e < c < b INSTRUMENT: P-E 301
LABORATORY BUREAU OF MINES PETROLEUM RES. CTR. BARTLESVILLE, OKLA.			

Figure 17 — Spectra of Hexamethyldisiloxane.

TABLE XVII

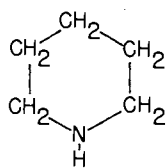
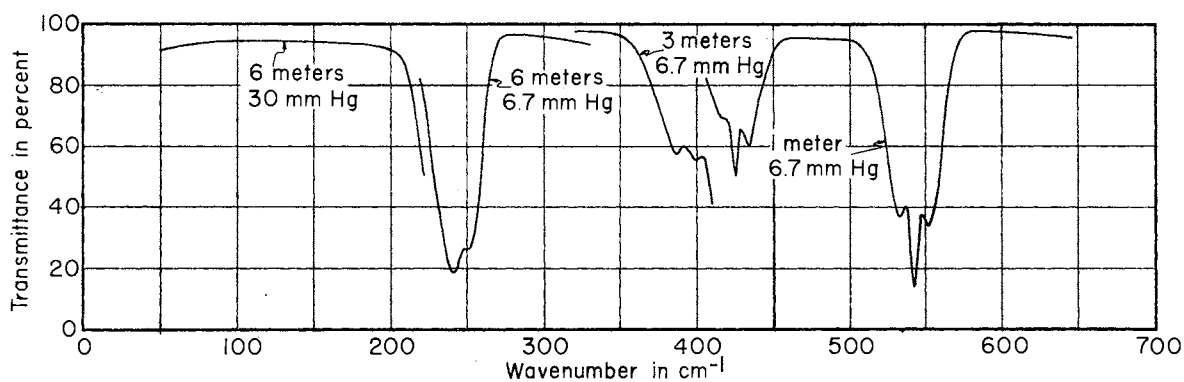
FAR INFRARED ABSORPTION MAXIMA FOR HEXAMETHYLDISILOXANE

Liquid or Solution	Vapor
220	217
247	246
330	329
	490
521	512
	546
618	619



COMPOUND	SOURCE AND PURITY	STATE: SOLUTION	SOLVENT: CYCLOPENTANE OR 2,2,4-TRIMETHYLPENTANE
PIPERIDINE	API RESEARCH PROJECT 52 B	TEMPERATURE: ROOM	CONCENTRATION: 5 %
$C_5H_{11}N$	99.94 ± 0.02 MOLE %	CELL LENGTH: AS INDICATED	INSTRUMENT: P-E 301

LABORATORY
BUREAU OF MINES
PETROLEUM RES. CTR.
BARTLESVILLE, OKLA.



COMPOUND	SOURCE AND PURITY	STATE: VAPOR	PRESSURE: AS INDICATED
PIPERIDINE	API RESEARCH PROJECT 52 B	TEMPERATURE: ROOM	INSTRUMENT: P-E 301
$C_5H_{11}N$	99.94 ± 0.02 MOLE %	CELL LENGTH: AS INDICATED	

LABORATORY
BUREAU OF MINES
PETROLEUM RES. CTR.
BARTLESVILLE, OKLA.

Figure 18 — Spectra of Piperidine.

TABLE XVIII
FAR INFRARED ABSORPTION MAXIMA FOR PIPERIDINE

Liquid or Solution	Vapor
248	241
	250
389	386
401	399
428	{ 417 P 425 Q 434 R
444	
542	{ 533 P 542 Q 551 R

Frequency Shifts between Liquid and Vapor States

In most vibrational analyses, values for the lowest frequencies have been obtained from Raman spectra since there have been relatively few far infrared spectrometers in use. Since it is difficult to obtain the Raman spectra of gases, the spectra obtained for the liquid state generally have been used, with the assumption that the vibrational frequencies are the same in the liquid and vapor states. The justification for this practice was that when comparisons were made of higher frequencies (wavenumber greater than 300 cm^{-1}) in the liquid and vapor states, the differences found were small and seldom important thermodynamically.

The use of liquid-state spectra was a matter of practical necessity in many cases. For example, if the substance had too low a vapor pressure for the vapor-state infrared spectrum to be determined conveniently, or if the substance had fundamentals that were infrared inactive but Raman active, only Raman data could be used, and as stated above, most of the Raman data were for the liquid state. The use of Raman data was certainly a necessity before the introduction of grating spectrometers, when infrared measurements were limited to the prism region above 250 cm^{-1} .

For many years the assumption that the low frequencies (wavenumber less than 250 cm^{-1}) were substantially the same in the liquid and vapor states was not questioned seriously or tested experimentally, and liquid-state frequencies often were used to calculate ideal-gas thermodynamic properties. Comparisons with calorimetrically determined values of entropy usually did not help in testing the assumption, because most molecules with low frequencies also have one or more restricted

internal rotations. Any errors in the low frequencies were then absorbed in the value of the barrier height calculated from the observed entropy and were not apparent. Only in studies of molecules with free or nearly free internal rotation was evidence finally obtained that low frequencies may differ considerably in the liquid and vapor states. For dimethylacetylene, toluene, 2-methylpyridine, and 3-methylpyridine, entropy discrepancies were observed when liquid-state values of low frequencies were used (3,4,5,6). These discrepancies were resolved when the far infrared spectra in the vapor state were determined with grating instruments and the low frequencies were shown to differ significantly from their values in the liquid state. Since the low frequencies are the ones that contribute most to the thermodynamic functions, an error of only a few wavenumbers can result in a significant discrepancy between observed and calculated entropy values. The frequencies in the vapor state were found to be lower, so the direction of the shift is opposite to that usually observed with higher-frequency vibrations.

Fateley and coworkers, whose work in far infrared spectroscopy initially demonstrated the phenomenon of liquid-vapor shifts for toluene and the methylpyridines, have reported shifts of low frequencies for a variety of compounds (7). Actually, these are not the only observations of such shifts. Literature values of low frequencies determined in both states, whose review is beyond the scope of this thesis, reveal other examples of shifts, whose significance was not appreciated earlier.

Results. - Liquid-vapor frequency shifts could be measured for thirteen of the eighteen compounds studied in this investigation. The wavenumber for vapor and liquid (or solution in cyclopentane) and the extent of the shift are summarized in Table XIX.

TABLE XIX
 WAVENUMBERS FOR VAPOR AND LIQUID (OR SOLUTION)
 AND EXTENT OF SHIFT

Compound	Vapor	Liquid	$\Delta\nu$
2-Methylthiophene	225	234	-9
3-Methylthiophene	226	235	-9
4-Methylpyridine	203	210	-7
1-Methylpyrrole	186	198	-12
1,4-Dimethylbenzene ^a	132	152	-20
1,4-Difluorobenzene ^b	157	166	-9
1,3-Difluorobenzene	224	230	-6
2,4-Dimethyl-3-thiapentane	74	83	-9
Tetramethyllead	120	130	-10
Piperidine	241	248	-7
2,3-Dithiabutane	101	115	-14
Thiacyclopentane	100	105	-5
2-Propanethiol	185	186	-1

^a Fateley, et al. (7) give: vapor, 132 cm^{-1} ; liquid, 149 \pm cm^{-1} .

^b Green, et al. (9) give: vapor, 163 cm^{-1} ; liquid, 164 cm^{-1} .

The low fundamentals for three compounds were observed in the infrared spectra of the liquid, but the corresponding bands were not observed in the vapor spectra because the intensity was too low. These compounds and the liquid-state wave-

numbers of the low fundamentals are: 1,2-difluorobenzene, 198 cm^{-1} ; benzene-thiol, 186 cm^{-1} ; and benzotrifluoride, 140 cm^{-1} . The Si-O-Si bending mode of hexamethyldisiloxane had an intensity too low to be observed in either the vapor or liquid infrared spectrum. Calorimetric data indicate a vapor-state wavenumber of about 102 cm^{-1} for this mode (8). A shift also could not be determined for cyclohexanethiol because of overlapping of two bands in the liquid, as shown in Figure 13.

Discussion. - A shift of the lowest fundamental frequency between liquid and vapor states has been observed for most of the compounds studied in this investigation. Since the vapor-state frequencies are needed for studies in molecular energetics, and since the liquid-state frequencies are known for many molecules, a theory that would give accurate predictions of the shifts would be quite valuable. However, such a theory is not likely to be presented in the near future for several reasons. The frequency shift must be due to intermolecular effects in the liquid which are not present in the vapor. These may be both electrostatic and steric effects, and must depend on the shape and size of the molecule and the relative positions of the molecules in the liquid. Therefore, it does not seem possible at present to make quantitative predictions of frequency shifts. However, if the wavenumber of a fundamental vibration of a molecule is below about 250 cm^{-1} , the liquid and vapor-state values will probably be different, with the vapor-state value being the lower of the two.

The first four compounds in Table XIX are methyl derivatives of planar ring compounds, and the bands listed are for out-of-plane methyl bending modes. The shifts range from -7 to -12 cm^{-1} . This is the same range as found by Fateley, et

al. (7), for similar modes of related compounds. They find $\Delta\nu$ (2-methylpyridine) = $-12 \pm 2 \text{ cm}^{-1}$ and $\Delta\nu$ (3-methylpyridine) = $-10 \pm 2 \text{ cm}^{-1}$. Table XIX gives $\Delta\nu$ (4-methylpyridine) = -7 cm^{-1} , so there is a small effect of position of the methyl group.

The next three compounds in Table XIX are disubstituted benzenes, and the bands listed are for modes involving out-of-plane bending of the substituents. Comparison of the results for 1,4-dimethylbenzene and 1,4-difluorobenzene shows the greater shift occurs for the methyl derivative. This may be due to the difference in size of the two groups, but other factors are involved, because the same size shift was observed for m-fluorotoluene and m-chlorotoluene by Fateley, et al. (7). The series of difluorobenzenes shows a small effect of position of substituents.

The bands listed for the next three compounds in Table XIX, 2,4-dimethyl-3-thiapentane, tetramethyllead, and piperidine, are for skeletal bending or torsional modes. The value of $\Delta\nu$ listed for piperidine is somewhat ambiguous, since the complexity of the spectrum suggests that both the axial and equatorial conformations with respect to the amine hydrogen are present in appreciable concentration, and the low wavenumber bands of liquid and vapor may be a superposition of one or more bands from each of the conformations.

The last three compounds in Table XIX have low fundamentals involving restricted internal rotation (pseudo-rotation for thiacyclopentane). Although a shift could not be determined for cyclohexanethiol, it seemingly is small.

Study of Restricted Internal Rotation by Infrared Spectroscopy

Restricted internal rotation involving an unsymmetrical rotor gives rise to torsional frequencies that are infrared active. Also, restricted internal rotation involving a symmetrical rotor can give rise to infrared absorption if there is any interaction between the torsion and another mode in which the dipole moment is changed. The height of the barrier restricting the internal rotation and the reduced moment of inertia for internal rotation determine the value of the torsional frequency.

If a rotor such as $-SH$ is attached to a three-fold symmetrical frame, e.g., $-CH_3$, the rotation is opposed by a three-fold symmetrical potential barrier given by

$$V(\varphi) = 1/2 V_3 (1 - \cos 3\varphi) + 1/2 V_6 (1 - \cos 6\varphi) + \dots \quad (1)$$

in which φ is the torsional angle. If all terms higher than V_3 are ignored, substitution of equation (1) into the torsional wave equation gives the Mathieu equation, solutions of which have been studied rather thoroughly.

For a three-fold symmetric barrier that is sufficiently high, the torsional energy levels are triply degenerate. If the barrier is sufficiently low, the energy levels are split into a nondegenerate (A) and a doubly degenerate (E) sublevel. The two sublevels very nearly coincide for the lowest quantum state, but become split for higher states, with the splitting increasing with increasing torsional quantum number.

2-Propanethiol. - In the spectrum of this compound, a band with distinct PQR structure occurs at 185 cm^{-1} , and a weak band with the same contour occurs at

238 cm^{-1} , as shown in Figure 12. This compound exists as two rotational isomers of C_1 and C_3 symmetry. If the barrier to internal rotation of the thiol group is three-fold symmetrical, the concentration of the C_1 form would be twice that of the C_3 form. Moreover, thiol torsion in the C_1 form involves a change of dipole moment in the direction favorable to a prominent Q branch of the infrared band. Presumably, then, the 185 cm^{-1} band is to be attributed to the C_1 form. There are two torsional modes involving the methyl groups, one of which would probably interact more with the thiol torsion and would be more intense. This mode gives rise to the band observed at 238 cm^{-1} . Theoretical energy levels have not been derived for the situation of an unsymmetrical top attached to an unsymmetrical frame; however, the levels that have been derived for a three-fold symmetrical top (10) may be used as a suitable approximation. The torsional energy from solution of Mathieu's equation is

$$\Delta E_{\nu\sigma} = 9/4 F \Delta b_{\nu\sigma} \quad (2)$$

In this equation, $b_{\nu\sigma}$ is an eigenvalue of the Mathieu equation, F is given by $F = h^2/8\pi^2 I_r$, and I_r is the reduced moment of inertia for internal rotation.

From the $0 \rightarrow 1$ (E) transition (185 cm^{-1} for thiol torsion and 238 cm^{-1} for methyl torsion), $\Delta b_{\nu\sigma} = b_{0E} - b_{1E}$ can be calculated and from this a dimensionless parameter, s , can be obtained from tables of solutions for the Mathieu equation. The barrier height can then be calculated from the equation

$$V = 9/4 F s \quad (3)$$

The approximate reduced moments of inertia for the thiol and methyl rotations were calculated from equation (1b) of reference (11) to be:

$I_r(\text{methyl}) = 5.22 \times 10^{-40} \text{ g cm}^2$; $I_r(\text{thiol}) = 2.76 \times 10^{-40} \text{ g cm}^2$. The barrier height for the observed methyl torsion was then determined from tables of eigenvalues of the Mathieu equation (12) to be $3.73 \text{ kcal mole}^{-1}$. A barrier height of $1.42 \text{ kcal mole}^{-1}$ was calculated for the thiol torsion. These values agree reasonably well with the values 3.95 and $1.39 \text{ kcal mole}^{-1}$ obtained from calorimetric data (13). The differences indicate an interaction between the torsional modes.

The first upper-stage band for the C_1 form thiol torsion [$1 \rightarrow 2$ (E)] would be predicted at 160 cm^{-1} , and the fundamental and first upper-stage band for the C_s form [$0 \rightarrow 1$ (A) and $1 \rightarrow 2$ (A)] would be predicted at 188 and 134 cm^{-1} , respectively. A weak shoulder observed at about 160 cm^{-1} may be the first of these predicted bands, but the other two are not observed.

Cyclohexanethiol. - The torsional fundamental in cyclohexanethiol is a broad, structureless band centered at 178 cm^{-1} , as shown in Figure 13. It is the composite of bands for the four conformations, axial- C_1 , axial- C_s , equatorial- C_1 , and equatorial- C_s . The immediate environment of the thiol group in either the axial or equatorial forms of cyclohexanethiol is very similar to that in 2-propanethiol, so nearly the same barrier height for thiol torsion would be expected. For the same barrier height, the wavenumber of the band would be expected to be slightly less for cyclohexanethiol than for 2-propanethiol, since the reduced moments of inertia for thiol torsion are larger for the various conformations of cyclohexanethiol than for 2-propanethiol. Also, the apparent band center could be lower than the

average center of the individual bands. It is understandable, therefore, that the band observed for cyclohexanethiol at 178 cm^{-1} is 7 cm^{-1} lower than the corresponding band for 2-propanethiol.

2,3-Dithiabutane. - In 1958, D. W. Scott and coworkers (14) calculated from vapor-state thermodynamic properties that the potential barrier restricting torsion about the S-S bond of 2,3-dithiabutane corresponds to a wavenumber of 98 cm^{-1} for the torsional mode. The observed wavenumber from the Raman spectrum of the liquid was about 120 cm^{-1} . This was a puzzling discrepancy before the possibility of large frequency shifts between vapor and liquid was appreciated. The observed shift shown in Figure 10 provides the explanation. The values for the vapor and liquid are 101 and 115 cm^{-1} . The thermodynamic and spectroscopic values for the vapor state thus agree within their experimental uncertainty.

Thiacyclopentane. - The results for thiacyclopentane constitute the first direct observation of the lowest oscillational fundamental. Calorimetric data for this compound have been interpreted by assuming for the restricted pseudo-rotation a cosine-type barrier of $2800 \text{ cal mole}^{-1}$ height and effective moment of inertia, I , of $10.66 \times 10^{-40} \text{ g cm}^2$ (15).

The perturbed harmonic oscillator approximation reduces to

$$\sqrt{\nu} = 0.188355 \times 10^{12} \nu \sqrt{2I}/n + 2.6357 \times 10^{-28} n/\sqrt{2I} (1 + 1) \quad (4)$$

in which $\nu = 0.69469 \times 10^{-16} V$, V is the barrier height in cal mole^{-1} , I is the vibrational quantum number, n is the number of potential minima, and ν is in cm^{-1} .

For the model given above, the difference between the ground and first excited

states is calculated from equation (4) to be 99 cm^{-1} . The agreement with the observed value of 100 cm^{-1} still leaves difficulties, however, because with the cosine-type barrier, upper-stage bands would be spaced about 2.6 cm^{-1} , and the composite band probably would have a smeared-out contour. The 100 cm^{-1} band actually has a well-defined contour indicative of upper-stage bands nearly coinciding with the fundamental. Costain (16) also finds from microwave observations that this vibration is nearly harmonic through the first five energy levels. These observations indicate that the lower part of the potential function for hindered pseudo-rotation is more nearly parabolic than the assumed cosine function.

Low Fundamentals

As is well known, the selection rules governing absorption of radiation in Raman and infrared spectroscopy are different, so bands may be observed in infrared spectra that are not allowed in Raman spectra. Even when symmetry permits observation of a band in both types of spectra, the intensity of a band in the two types are unrelated, so a band may be observed in one and yet have an intensity in the other that is too low to be observed. In this investigation, several bands were observed that had not been observed in the Raman spectra.

The Raman spectrum of 2,4-dimethyl-3-thiapentane in the liquid state has been observed, with the lowest band reported at 290 cm^{-1} . The isopropyl torsional modes are apparently too weak to be observed in the Raman spectrum, but one was observed in this investigation, as shown in Figure 9. The wavenumber values are 74 cm^{-1} in the vapor and 83 cm^{-1} in the liquid. This is the lowest fundamental observed for any of the compounds studied in this investigation, although a

difference band was observed at 66 cm^{-1} in the liquid spectrum and 63 cm^{-1} in the vapor spectrum of benzotrifluoride.

Raman observations also failed to detect the thiol and methyl torsional frequencies of 2-propanethiol and the thiol torsional frequency of cyclohexanethiol. The thiol torsional frequencies were observed in this investigation as the strongest bands in the $50\text{--}650\text{ cm}^{-1}$ infrared region, and a methyl torsional mode of 2-propanethiol was observed as a weak band. The pseudo-rotational mode of thiacyclopentane also was observed in this investigation, but not in the Raman spectrum.

Low-frequency infrared bands which are forbidden by selection rules in the Raman effect were observed for 1,4-dimethylbenzene and 1,4-difluorobenzene.

CHAPTER III

VIBRATIONAL ANALYSIS BY DIGITAL COMPUTER

In this chapter will be given a general description of the methods used in the normal-coordinate calculations and a detailed account of the normal-coordinate analysis for tetramethyllead and 2,4-dimethyl-3-thiapentane. The calculations were done with an IBM 7094 computer at the Los Alamos Scientific Laboratory.

Methods

The calculations were done with G-Matrix Evaluation Program SD-9064-I, Z-Matrix Evaluation Program SD-9080-I, and Vibrational Secular Equation Program SD-9032-IV.

The vibrational problem is set up by the Wilson FG method (17). If R is a set of internal valence coordinates, the potential energy of the vibrating molecule may be written as

$$2V = R'FR \quad (5)$$

and the kinetic energy is

$$2T = \dot{R}'G^{-1}\dot{R} \quad (6)$$

in which F is the force constant matrix and G is the inverse kinetic energy matrix. A transformation L is found such that the potential and kinetic energies are diagonalized. L is defined by

$$R = LQ \quad (7)$$

The Q 's are the normal coordinates. Substitution of (7) into (5) and (6) gives

$$2V = Q'L'FLQ = Q'\Lambda Q \quad (8)$$

from which it follows that

$$L'FL = \Lambda \quad (9)$$

and

$$2T = \dot{Q}'L'G^{-1}L\dot{Q} = \dot{Q}'E\dot{Q} \quad (10)$$

from which we get

$$L'G^{-1}L = E \quad (11)$$

in which E is a unit matrix. Equation (11) gives

$$L' = L^{-1}G \quad (12)$$

and substitution of this in (9) gives

$$GFL = L\Lambda \quad (13)$$

This is the secular equation. Λ is a diagonal matrix whose elements are

$$\Lambda_{ii} = \lambda_i = 4\pi^2 c^2 \nu_i^2 / N, \text{ in which } \nu_i \text{ are the vibrational frequencies.}$$

In terms of symmetry coordinates, the potential and kinetic energies are

$$2V = S' \mathcal{F} S \quad (14)$$

and

$$2T = \dot{S}' G^{-1} \dot{S} \quad (15)$$

If U is the transformation from internal coordinates to symmetry coordinates, then the symmetry coordinates are given by

$$S = UR \quad (16)$$

From equations (14), (15), and (16), it follows that

$$\mathcal{F} = UFU' \quad (17)$$

and

$$\mathcal{G} = UGU' \quad (18)$$

Also,

$$\mathcal{L} = UL \quad (19)$$

so the secular equation in terms of symmetry coordinates is

$$\mathcal{G} \mathcal{L} = \mathcal{L} \Lambda \quad (20)$$

If B is the transformation from cartesian displacement coordinates, x , to internal coordinates, R , i.e.,

$$R = Bx \quad (21)$$

then G is given by

$$G = BM^{-1}B' \quad (22)$$

in which M^{-1} is a diagonal matrix of the reciprocal masses. The B matrix elements are computed by the Wilson s -vector technique. The elements of the diagonal matrix Λ are calculated from the observed frequencies. This leaves only the force constant matrix F to be determined. In practice the determination of the force constants from the observed frequencies is a much more difficult problem than the reverse procedure. Therefore initial estimates of the force constants are made and the λ 's are calculated with these estimated values.

Let F_o be the initial F matrix and Λ_o and L_o the computed eigenvalues and eigenvectors for the problem

$$GF_o L_o = L_o \Lambda_o \quad (23)$$

We want to refine F_o by the amount ΔF so that the observed frequency parameters are obtained from the solution of

$$G(F_o + \Delta F) - \lambda E = 0 \quad (24)$$

If we expand $\Delta \Lambda = \Lambda_{obs} - \Lambda_{calc}$ in terms of the force constants and keep only the linear terms, we have

$$\vec{\Delta \lambda} = J \vec{\Delta F} \quad (25)$$

in which $\vec{\Delta \lambda}$ is a column of $\lambda_{obs} - \lambda_{calc}$ arranged in a convenient order, $\vec{\Delta F}$ is a column of corrections to the F matrix, and J is the matrix of the force constant Jacobian. It can be shown (18) that

$$\Delta \lambda_i = \sum_{k,m} (L_o)_{ik} (L_o)_{mk} \Delta F_{mk} \quad (26)$$

The best correction to F_o is found by solving the least squares equation

$$J' P \vec{\Delta \lambda} = J' P J \vec{\Delta F} \quad (27)$$

in which P is a diagonal weighting matrix giving the confidence in each observed λ .

The force constant matrix is set up in terms of Urey-Bradley force constants and the transformation, Z, from Urey-Bradley space to internal coordinate space

$$F = Z \vec{\Phi} \quad (28)$$

is found. $\vec{\Phi}$ is a column of independent Urey-Bradley force constants. Provision is made in the program for the introduction of non-Urey-Bradley interaction constants. Substitution of (28) into (25) gives

$$\vec{\Delta\lambda} = \mathbf{JZ}\vec{\Delta\Phi} \quad (29)$$

and the least squares equation becomes

$$(\mathbf{JZ})' \mathbf{P} \vec{\Delta\lambda} = (\mathbf{JZ})' \mathbf{P} (\mathbf{JZ}) \vec{\Delta\Phi} \quad (30)$$

After $\vec{\Delta\Phi}$ is determined, the correction to the F matrix is computed by

$$\vec{\Delta F} = \mathbf{Z} \vec{\Delta\Phi} \quad (31)$$

The equation

$$\mathbf{G}(\mathbf{F} + \vec{\Delta F})\mathbf{L} = \mathbf{L}\Lambda \quad (32)$$

is solved and the cycle repeated until the λ 's converge to the observed frequency parameters, or until further refinement produces no significant changes in the force constants. Of course, if the calculated λ 's diverge, one must look for changes in the force constants or the force field.

The Z matrix is used to calculate the potential energy distribution for each vibration among the elements of Φ . The potential energy distribution is defined as (19)

$$\text{PE} = \Lambda^{-1} \mathbf{JZ}\Phi \quad (33)$$

in which Φ is now a diagonal matrix of the elements of the column $\vec{\Phi}$.

The matrix GF is not symmetric, so the solution of the secular equation is accomplished by the solution of two symmetric problems. This allows the computer to remove the redundancies.

This brief summary has been restricted to the methods that were applied to the tetramethyllead and 2,4-dimethyl-3-thiapentane molecules. Actually, Dr. Schachtschneider's programs provide for other things that have not been mentioned here, e.g., mean amplitudes of vibration and Coriolis coupling coefficients.

Tetramethyllead

A study of the tetramethyllead molecule was desirable, even though it had been the subject of several investigations (20 - 28), because these investigations left the vibrational assignment still in doubt. In particular, the C-Pb-C bending frequencies have been based on the Raman spectrum of the liquid, and Figure 14 shows that the \underline{f}_2 bending frequency is different in the vapor and liquid states. One would also expect the \underline{e} bending frequency to be different in the two states. Also, different authors assigned $\nu_5(e)$ and $\nu_6(e)$ (Table XXIII) to different bands. The present calculations were done in order to estimate the wavenumbers of the Raman and infrared inactive type \underline{f}_1 vibrations and the type \underline{e} vibrations.

For \underline{T}_d point-group symmetry and if the torsional modes are excluded, the normal vibrations of tetramethyllead are distributed as follows:

$$3\underline{a}_1 + 4\underline{e} + 3\underline{f}_1 + 7\underline{f}_2$$

The \underline{a}_1 , \underline{e} , and \underline{f}_2 modes are Raman active, whereas only the \underline{f}_2 modes are infrared active. The two C-Pb-C bending frequencies are of species \underline{e} and \underline{f}_2 , and so both are permitted by selection rules in the Raman effect. However, in the pertinent region of the Raman spectrum, only one very broad, asymmetric band is observed with a maximum intensity at about 132 cm^{-1} . In recent assignments, this band has been assumed to be double and to include both C-Pb-C bending frequencies. For example, Overend and Scherer (29) assign the values 130 and 140 cm^{-1} to the \underline{e} and \underline{f}_2 bending modes, whereas Lippincott and Tobin (25) assign to these modes the values 130 and 145 cm^{-1} . These authors used the value 1400 cm^{-1} for the asymmetric methyl deformation mode $\nu_5(e)$ and 700 cm^{-1} for the methyl

rocking mode ν_6 (e). Sheline and Pitzer (23) assign to ν_5 and ν_6 the values 1453 and 767 cm^{-1} , and they assign 102 cm^{-1} to the C-Pb-C bending mode ν_7 (e) because this gave the best fit with combination bands.

Table XX lists the bands observed for tetramethyllead vapor in the far infrared region and their present interpretation.

TABLE XX
FAR INFRARED BANDS OF TETRAMETHYLLEAD VAPOR

cm^{-1}	Interpretation
120	Fundamental \underline{f}_2
243	$2 \times 120 = 240 \underline{A}_1 + \underline{E} + \underline{F}_2$
355	$476 - 120 = 356 \underline{A}_1 + \underline{E} + \underline{F}_1 + \underline{F}_2$
468 P sh. 476 Q 483 R	Fundamental \underline{f}_2
580	$460(\underline{a}_1) + 120 = 580 \underline{F}_2$
599	$476 + 120 = 596 \underline{A}_1 + \underline{E} + \underline{F}_1 + \underline{F}_2$

The distorted molecule was described by 46 internal coordinates, with the internal rotations being ignored. An example of each type of coordinate and the method of indexing are shown in Figure 19.

From these internal coordinates the following symmetry coordinates were constructed for the $3\underline{a}_1 + 4\underline{e} + 3\underline{f}_1 + 7\underline{f}_2$ normal modes:

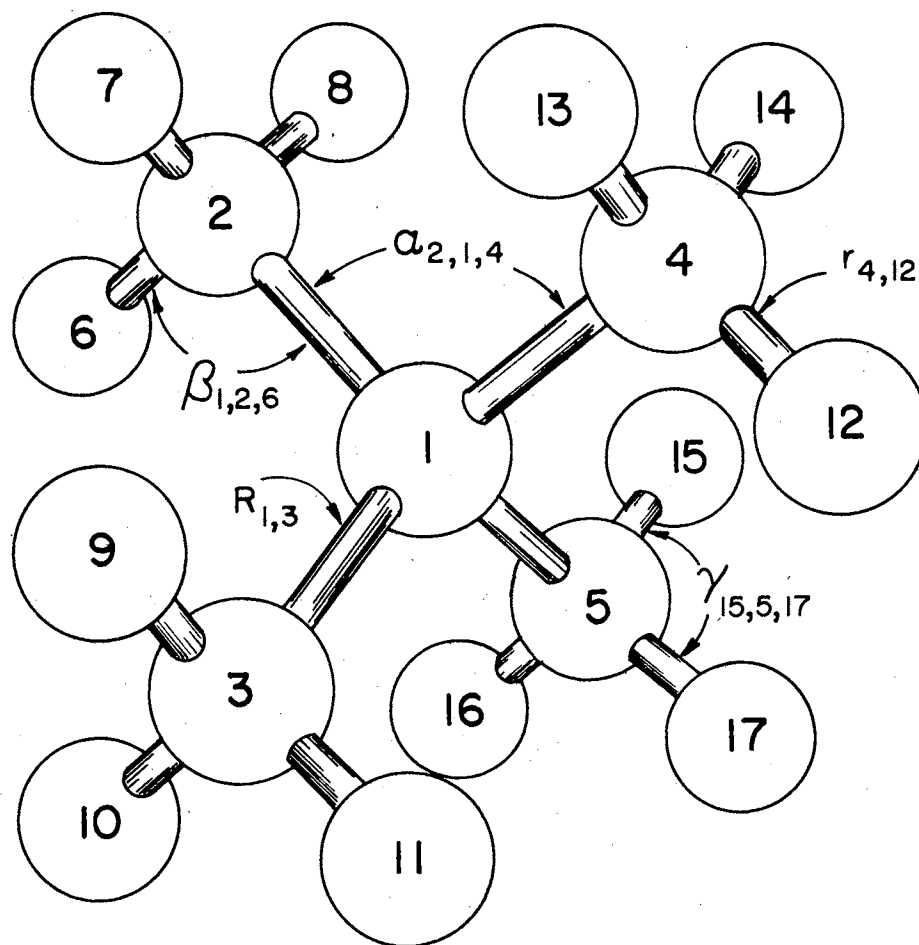


Figure 19 - Internal Coordinates of Tetramethyllead

$$S_1^{a1} = \Delta(R_{1,2} + R_{1,3} + R_{1,4} + R_{1,5})/2$$

$$S_2^{a1} = \Delta(r_{2,6} + r_{2,7} + r_{2,8} + r_{3,9} + r_{3,10} + r_{3,11} + r_{4,12} + r_{4,13} + r_{4,14} + r_{5,15} + r_{5,16} + r_{5,17})/\sqrt{12}$$

$$S_3^{a1} = \Delta(\alpha_{2,1,3} + \alpha_{2,1,4} + \alpha_{2,1,5} + \alpha_{3,1,4} + \alpha_{3,1,5} + \alpha_{4,1,5})/\sqrt{6}$$

$$S_4^{a1} = \Delta(\beta_{1,2,6} + \beta_{1,2,7} + \beta_{1,2,8} + \beta_{1,3,9} + \beta_{1,3,10} + \beta_{1,3,11} + \beta_{1,4,12} + \beta_{1,4,13} + \beta_{1,4,14} + \beta_{1,5,15} + \beta_{1,5,16} + \beta_{1,5,17})/\sqrt{12}$$

$$S_5^{a1} = \Delta(\gamma_{6,2,7} + \gamma_{6,2,8} + \gamma_{7,2,8} + \gamma_{9,3,10} + \gamma_{9,3,11} + \gamma_{10,3,11} + \gamma_{12,4,13} + \gamma_{12,4,14} + \gamma_{13,4,14} + \gamma_{15,5,16} + \gamma_{15,5,17} + \gamma_{16,5,17})/\sqrt{12}$$

$$S_{1a}^e = \Delta(2r_{2,6} - r_{2,7} - r_{2,8} + 2r_{3,9} - r_{3,10} - r_{3,11} + 2r_{4,12} - r_{4,13} - r_{4,14} - r_{5,16} - r_{5,17})/\sqrt{24}$$

$$S_{1b}^e = \Delta(-\alpha_{2,1,3} + 2\alpha_{2,1,4} - \alpha_{2,1,5} - \alpha_{3,1,4} + 2\alpha_{3,1,5} - \alpha_{4,1,5})/\sqrt{12}$$

$$S_{1c}^e = \Delta(2\beta_{1,2,6} - \beta_{1,2,7} - \beta_{1,2,8} + 2\beta_{1,3,9} - \beta_{1,3,10} - \beta_{1,3,11} + 2\beta_{1,4,12} - \beta_{1,4,13} - \beta_{1,4,14} + 2\beta_{1,5,15} - \beta_{1,5,16} - \beta_{1,5,17})/\sqrt{24}$$

$$S_{1d}^e = \Delta(-\gamma_{6,2,7} - \gamma_{6,2,8} + 2\gamma_{7,2,8} - \gamma_{9,3,10} - \gamma_{9,3,11} + 2\gamma_{10,3,11} - \gamma_{12,4,13} - \gamma_{12,4,14} + 2\gamma_{13,4,14} - \gamma_{15,5,16} - \gamma_{15,5,17} + 2\gamma_{16,5,17})/\sqrt{24}$$

$$S_{2a}^e = \Delta(-r_{2,7} + r_{2,8} - r_{3,10} + r_{3,11} + r_{4,13} - r_{4,14} + r_{5,16} - r_{5,17})/\sqrt{8}$$

$$S_{2b}^e = \Delta(\alpha_{2,1,3} - \alpha_{2,1,5} - \alpha_{3,1,4} + \alpha_{4,1,5})/2$$

$$S_{2c}^e = \Delta(-\beta_{1,2,7} + \beta_{1,2,8} - \beta_{1,3,10} + \beta_{1,3,11} + \beta_{1,4,13} - \beta_{1,4,14} + \beta_{1,5,16} - \beta_{1,5,17})/\sqrt{8}$$

$$S_{2d}^e = \Delta(\gamma_{6,2,7} - \gamma_{6,2,8} + \gamma_{9,3,10} - \gamma_{9,3,11} - \gamma_{12,4,13} + \gamma_{12,4,14} - \gamma_{15,5,16} + \gamma_{15,5,17})/\sqrt{8}$$

$$S_{1a}^{f1} = \Delta(2r_{2,6} - r_{2,7} - r_{2,8} - r_{3,10} + r_{3,11} - 2r_{4,12} + r_{4,13} + r_{4,14} - r_{5,16} + r_{5,17})/4$$

$$S_{1b}^{f1} = \Delta(2\beta_{1,2,6} - \beta_{1,2,7} - \beta_{1,2,8} - \beta_{1,3,10} + \beta_{1,3,11} - 2\beta_{1,4,12} + \beta_{1,4,13} + \beta_{1,4,14} - \beta_{1,5,16} + \beta_{1,5,17})/4$$

$$S_{1c}^{f1} = \Delta(-\gamma_{6,2,7} - \gamma_{6,2,8} + 2\gamma_{7,2,8} + \gamma_{9,3,10} - \gamma_{9,3,11} + \gamma_{12,4,13} + \gamma_{12,4,14} - 2\gamma_{13,4,14} + \gamma_{15,5,16} - \gamma_{15,5,17})/4$$

$$S_{2a}^{f1} = \Delta(r_{2,7} - r_{2,8} - 2r_{3,9} + r_{3,10} + r_{3,11} + r_{4,13} - r_{4,14} + 2r_{5,15} - r_{5,16} - r_{5,17})/4$$

$$S_{2b}^{f1} = \Delta(\beta_{1,2,7} - \beta_{1,2,8} - 2\beta_{1,3,9} + \beta_{1,3,10} + \beta_{1,3,11} + \beta_{1,4,13} - \beta_{1,4,14} + 2\beta_{1,5,15} - \beta_{1,5,16} - \beta_{1,5,17})/4$$

$$S_{2c}^{f1} = \Delta(-\gamma_{6,2,7} + \gamma_{6,2,8} + \gamma_{9,3,10} + \gamma_{9,3,11} - 2\gamma_{10,3,11} - \gamma_{12,4,13} + \gamma_{12,4,14} - \gamma_{15,5,16} - \gamma_{15,5,17} + 2\gamma_{16,5,17})/4$$

$$S_{3a}^{f1} = \Delta(r_{2,7} - r_{2,8} - r_{3,10} + r_{3,11} - r_{4,13} + r_{4,14} + r_{5,16} - r_{5,17})/\sqrt{8}$$

$$S_{3b}^{f_1} = \Delta(\beta_{1,2,7} - \beta_{1,2,8} - \beta_{1,3,10} + \beta_{1,3,11} - \beta_{1,4,13} + \beta_{1,4,14} + \beta_{1,5,16} - \beta_{1,5,17})/\sqrt{8}$$

$$S_{3c}^{f_1} = \Delta(-\gamma_{6,2,7} + \gamma_{6,2,8} + \gamma_{9,3,10} - \gamma_{9,3,11} + \gamma_{12,4,13} - \gamma_{12,4,14} - \gamma_{15,5,16} + \gamma_{15,5,17})/\sqrt{8}$$

$$S_{1a}^{f_2} = \Delta(R_{1,2} - R_{1,3} + R_{1,4} - R_{1,5})/2$$

$$S_{1b}^{f_2} = \Delta(r_{2,6} + r_{2,7} + r_{2,8} - r_{3,9} - r_{3,10} - r_{3,11} + r_{4,12} + r_{4,13} + r_{4,14} - r_{5,15} - r_{5,16} - r_{5,17})/\sqrt{12}$$

$$S_{1c}^{f_2} = \Delta(2r_{2,6} - r_{2,7} - r_{2,8} - 2r_{3,9} + r_{3,10} + r_{3,11} + 2r_{4,12} - r_{4,13} - r_{4,14} - 2r_{5,15} + r_{5,16} + r_{5,17})/\sqrt{24}$$

$$S_{1d}^{f_2} = \Delta(\alpha_{2,1,4} - \alpha_{3,1,5})/\sqrt{2}$$

$$S_{1e}^{f_2} = \Delta(\beta_{1,2,6} + \beta_{1,2,7} + \beta_{1,2,8} - \beta_{1,3,9} - \beta_{1,3,10} - \beta_{1,3,11} + \beta_{1,4,12} + \beta_{1,4,13} + \beta_{1,4,14} - \beta_{1,5,15} - \beta_{1,5,16} - \beta_{1,5,17})/\sqrt{12}$$

$$S_{1f}^{f_2} = \Delta(2\beta_{1,2,6} - \beta_{1,2,7} - \beta_{1,2,8} - 2\beta_{1,3,9} + \beta_{1,3,10} + \beta_{1,3,11} + 2\beta_{1,4,12} - \beta_{1,4,13} - \beta_{1,4,14} - 2\beta_{1,5,15} + \beta_{1,5,16} + \beta_{1,5,17})/\sqrt{24}$$

$$S_{1g}^{f_2} = \Delta(\gamma_{6,2,7} + \gamma_{6,2,8} + \gamma_{7,2,8} - \gamma_{9,3,10} - \gamma_{9,3,11} - \gamma_{10,3,11} + \gamma_{12,4,13} + \gamma_{12,4,14} + \gamma_{13,4,14} - \gamma_{15,5,16} - \gamma_{15,5,17} - \gamma_{16,5,17})/\sqrt{12}$$

$$S_{1h}^{f_2} = \Delta(-\gamma_{6,2,7} - \gamma_{6,2,8} + 2\gamma_{7,2,8} + \gamma_{9,3,10} + \gamma_{9,3,11} - 2\gamma_{10,3,11} - \gamma_{12,4,13} - \gamma_{12,4,14} + 2\gamma_{13,4,14} + \gamma_{15,5,16} + \gamma_{15,5,17} - 2\gamma_{16,5,17})/\sqrt{24}$$

$$S_{2a}^{f_2} = \Delta(R_{1,2} - R_{1,4})/\sqrt{2}$$

$$S_{2b}^{f_2} = \Delta(r_{2,6} + r_{2,7} + r_{2,8} - r_{4,12} - r_{4,13} - r_{4,14})/\sqrt{6}$$

$$S_{2c}^{f_2} = \Delta(2r_{2,6} - r_{2,7} - r_{2,8} + 3r_{3,10} - 3r_{3,11} - 2r_{4,12} + r_{4,13} + r_{4,14} + 3r_{5,16} - 3r_{5,17})/\sqrt{48}$$

$$S_{2d}^{f_2} = \Delta(\alpha_{2,1,3} + \alpha_{2,1,5} - \alpha_{3,1,4} - \alpha_{4,1,5})/2$$

$$S_{2e}^{f_2} = \Delta(\beta_{1,2,6} + \beta_{1,2,7} + \beta_{1,2,8} - \beta_{1,3,9} - \beta_{1,3,10} - \beta_{1,3,11} + \beta_{1,4,12} + \beta_{1,4,13} + \beta_{1,4,14} - \beta_{1,5,15} - \beta_{1,5,16} - \beta_{1,5,17})/\sqrt{12}$$

$$S_{2f}^{f_2} = \Delta(2\beta_{1,2,6} - \beta_{1,2,7} - \beta_{1,2,8} - 2\beta_{1,3,9} + \beta_{1,3,10} + \beta_{1,3,11} + 2\beta_{1,4,12} - \beta_{1,4,13} - \beta_{1,4,14} - 2\beta_{1,5,15} + \beta_{1,5,16} + \beta_{1,5,17})/\sqrt{24}$$

$$S_{2g}^{f_2} = \Delta(\gamma_{6,2,7} + \gamma_{6,2,8} + \gamma_{7,2,8} - \gamma_{9,3,10} - \gamma_{9,3,11} - \gamma_{10,3,11} + \gamma_{12,4,13} + \gamma_{12,4,14} + \gamma_{13,4,14} - \gamma_{15,5,16} - \gamma_{15,5,17} - \gamma_{16,5,17})/\sqrt{12}$$

$$S_{2h}^{f_2} = \Delta(-\gamma_{6,2,7} - \gamma_{6,2,8} + 2\gamma_{7,2,8} + \gamma_{9,3,10} + \gamma_{9,3,11} - 2\gamma_{10,3,11} - \gamma_{12,4,13} - \gamma_{12,4,14} + 2\gamma_{13,4,14} + \gamma_{15,5,16} + \gamma_{15,5,17} - 2\gamma_{16,5,17})/\sqrt{24}$$

$$S_{3a}^{f_2} = \Delta(R_{1,3} - R_{1,5})/\sqrt{2}$$

$$S_{3b}^{f_2} = \Delta(r_{3,9} + r_{3,10} + r_{3,11} - r_{5,15} - r_{5,16} - r_{5,17})/\sqrt{6}$$

$$S_{3c}^{f_2} = \Delta(3r_{2,7} - 3r_{2,8} + 2r_{3,9} - r_{3,10} - r_{3,11} + 3r_{4,13} - 3r_{4,14} - 2r_{5,15} + r_{5,16} + r_{5,17})/\sqrt{48}$$

$$S_{3d}^{f_2} = \Delta(\alpha_{2,1,3} - \alpha_{2,1,5} + \alpha_{3,1,4} - \alpha_{4,1,5})/2$$

$$S_{3e}^{f_2} = \Delta(\beta_{1,3,9} + \beta_{1,3,10} + \beta_{1,3,11} - \beta_{1,5,15} - \beta_{1,5,16} - \beta_{1,5,17})/\sqrt{6}$$

$$S_{3f}^{f_2} = \Delta(3\beta_{1,2,7} - 3\beta_{1,2,8} + 2\beta_{1,3,9} - \beta_{1,3,10} - \beta_{1,3,11} + 3\beta_{1,4,13} - 3\beta_{1,4,14} - 2\beta_{1,5,15} + \beta_{1,5,16} + \beta_{1,5,17})/\sqrt{48}$$

$$S_{3g}^{f_2} = \Delta(\gamma_{9,3,10} + \gamma_{9,3,11} + \gamma_{10,3,11} - \gamma_{15,5,16} - \gamma_{15,5,17} - \gamma_{16,5,17})/\sqrt{6}$$

$$S_{3h}^{f_2} = \Delta(-3\gamma_{6,2,7} + 3\gamma_{6,2,8} - \gamma_{9,3,10} - \gamma_{9,3,11} + 2\gamma_{10,3,11} - 3\gamma_{12,4,13} + 3\gamma_{12,4,14} + \gamma_{15,5,16} + \gamma_{15,5,17} - 2\gamma_{16,5,17})/\sqrt{48}$$

The potential energy of the distorted molecule was described by a Urey-Bradley force field in the form

$$\begin{aligned} 2V = & \sum^{12} [2K_{CH}^1 r^0(\Delta r) + K_{CH}(\Delta r)^2] + \sum^4 [2K_{CPb}^1 R^0(\Delta R) + K_{CPb}(\Delta R)^2] \\ & + \sum^6 [2H_{CPbC}^1(\Delta\alpha) + H_{CPbC}(\Delta\alpha)^2] + \sum^{12} [2H_{PbCH}^1(\Delta\beta) + H_{PbCH}(\Delta\beta)^2] \\ & + \sum^{12} [2H_{HCH}^1(\Delta\gamma) + H_{HCH}(\Delta\gamma)^2] + \sum^{12} [2F_{HH}^1 q_{HH}^0(\Delta q_{HH}) + F_{HH}(\Delta q_{HH})^2] \\ & + \sum^{12} [2F_{HPb}^1 q_{HPb}^0(\Delta q_{HPb}) + F_{HPb}(\Delta q_{HPb})^2] \\ & + \sum^6 [2F_{CC}^1 q_{CC}^0(\Delta q_{CC}) + F_{CC}(\Delta q_{CC})^2] \end{aligned}$$

In the foregoing, q is the distance between the indicated nonbonded atoms. The equilibrium distances are denoted by r^0 , R^0 , q_{HH}^0 , q_{HPb}^0 , and q_{CC}^0 . This is the same force field that was used by Overend and Scherer (29). After re-

removal of the redundant coordinates, the potential energy expression contains the eight quadratic force constants, the linear constants F_{ij}^1 , and the intramolecular tensions κ_{CH_3} and κ_{Pb} .

Two calculations were made; in both, the F_{ij}^1 were constrained by the conventional relationship, $F_{ij}^1 = -0.1 F_{ij}$. In calculation I, the intramolecular tension κ_{CH_3} was constrained to zero, and in calculation II, H_{HCPb} was constrained to several values and the best value found. The force constants not constrained were adjusted to give the best least-squares agreement of calculated and observed wavenumbers by the method described at the beginning of this chapter.

Wong and Schomaker's (30) value for the Pb-C distance, 2.303 Å, was used, along with the currently accepted value for the C-H distance, 1.10 Å, and all angles were assumed to be tetrahedral.

The initial values of the force constants used in calculation I were taken mainly from Overend and Scherer (29). Ten observed wavenumbers were used, along with the value 117 cm^{-1} for the \underline{e} C-Pb-C bending mode. The method by which this value was obtained is described in Chapter IV. The ten observed wavenumbers are those for the three \underline{a}_1 and seven \underline{f}_2 vibrations, the \underline{e} values being excluded because of lack of convincing evidence as to their correct assignment. The 120 and 476 cm^{-1} values are the vapor-state infrared wavenumbers obtained in this research, and the higher \underline{f}_2 wavenumbers are the average of unpublished vapor-state infrared data from Jones and Sheppard of Cambridge University and from Carlos

Ellis of the Bartlesville Petroleum Research Center. The \underline{a}_1 values were taken from the vapor-state Raman data of Waters and Woodward (28).

The calculated wavenumbers are compared with the observed values in Table XXI.

TABLE XXI
OBSERVED AND CALCULATED WAVENUMBERS OF TETRAMETHYLLEAD

Obs	Calc I	Calc II	Obs	Calc I	Calc II
	\underline{a}_1			\underline{e}	
2929	2928	2928	----	3003	3003
1178	1171	1172	----	1451	1452
459	459	460	---	764	765
	\underline{f}_2		(117)	117	117
3003	3003	3003		\underline{f}_1	
2928	2928	2928	----	3003	3003
1452	1451	1452	----	1451	1452
1166	1175	1172	---	762	763
767	766	767			
476	476	475			
120	120	120			

Calculation I is similar in many respects to Overend and Scherer's, but quantitative agreement between the two sets of force constants could not be expected because of the differences in vibrational assignment. Table XXII shows that the two sets of force constants are qualitatively similar.

TABLE XXII

COMPARISON OF FORCE CONSTANTS FOR TETRAMETHYLLEAD
(K and F in units of md A^{-1} , H and χ in md A rad^{-2})

Force Constant	Overend and Scherer	Calc I	Calc II
K_{PbC}	0.723	0.644	1.570
K_{CH}	4.489*	4.485	4.741
H_{CPbC}	0.317	0.222	0.204
H_{HCPb}	-0.163	-0.266	0.418
H_{HCH}	0.495	0.520	0.517
F_{CC}	0.003	0.006	0.016
F_{HPb}	0.672	0.845	0.097
F_{HH}	0.100*	0.064	0.067
χ_{Pb}	0.108	0.053	0.053
χ_{CH_3}	-0.010*	0.000*	-0.111

* constrained

Especially noticeable in the set of force constants obtained in calculation I and that of Overend and Scherer are the negative value of H_{HCPb} and the large value for F_{HPb} . A negative force constant has no obvious physical meaning, and H_{HCPb} is negative in this case because F_{HPb} is so large and the two force constants are negatively correlated. Calculation II was made in order to obtain more reasonable values for these force constants.

Table XXI shows that the observed value of $\nu_2(\underline{a}_1) = 1178$ is higher than the observed value of $\nu_{14}(\underline{f}_2) = 1166$, whereas the calculated values are in the reverse order; $\nu_2(\text{calc}) = 1171$ and $\nu_{14}(\text{calc}) = 1175 \text{ cm}^{-1}$.

This could be a result of not including in the force field an interaction constant between the H-C-H and H-C-Pb bendings, so in calculation II, χ_{CH_3} was not constrained to zero as in calculation I.

The method by which the force constants that were used in calculation II were obtained is as follows. The force constant H_{HCPb} was constrained in three separate calculations to the values 0.0, 0.2, and 0.4 milli-dyne angstrom radian⁻² (md A rad⁻²). The sums of the weighted square errors of the eigenvalues were then plotted against H_{HCPb} and the minimum in this curve was found at $H_{\text{HCPb}} = 0.418 \text{ md A rad}^{-2}$. The values of the other force constants found in the three calculations then were plotted in the same manner as a function of H_{HCPb} and the curves extrapolated to obtain the force constant values corresponding to $H_{\text{HCPb}} = 0.418 \text{ md A rad}^{-2}$. The results are given in Table XXII.

The values of the force constants H_{HCPb} and F_{HPb} now seem to correspond more closely to physical reality. Also, Table XXI shows that $\nu_2(\text{calc})$ is 1172 and $\nu_{14}(\text{calc}) = 1172 \text{ cm}^{-1}$, so the change in these calculated wavenumbers is in the right direction, although not quite large enough in magnitude. However, the error in each of these two calculated values is only 6 cm^{-1} , or 0.5%, and it was not thought that this could be improved enough to warrant further calculations. This is the maximum error between calculated and observed wavenumbers.

Table XXIII gives the present assignment of wavenumbers to the approximate type of motion of the vibrating molecule, and Table XXIV gives the potential energy distribution among the force constants for each of the vibrations for which an observed wavenumber was used in the normal-coordinate calculations. The values in Table XXIV have been rounded to the nearest percent.

TABLE XXIII
VIBRATIONAL ASSIGNMENT FOR TETRAMETHYLLEAD

Approximate type of motion	Species			
	<u>a</u> ₁	<u>e</u>	<u>f</u> ₁	<u>f</u> ₂
CH ₃ asym stretch		3003(ν_4)	3003(ν_8)	3003(ν_{11})
CH ₃ sym stretch	2929(ν_1)			2928(ν_{12})
CH ₃ asym def		1452(ν_5)	1452(ν_9)	1452(ν_{13})
CH ₃ sym def	1178(ν_2)			1166(ν_{14})
CH ₃ rock		765(ν_6)	763(ν_{10})	767(ν_{15})
Pb-C stretch	459(ν_3)			476(ν_{16})
C-Pb-C def		117(ν_7)		120(ν_{17})

TABLE XXIV

POTENTIAL ENERGY DISTRIBUTION FOR TETRAMETHYLLEAD

	ν_i	cm^{-1}	K_{PbC}	K_{CH}	H_{CPbC}	H_{HCPb}	H_{HCH}	F_{CC}	F_{HPb}	F_{HH}	χ_{Pb}	χ_{CH_3}
a_1	1	2928		96					1	3		
	2	1178	3			49	64		8	4		-28
	3	459	79					3	17			
e	7	117			94			14			-9	
f_2	11	3003		98					1	1		
	12	2928		96					1	3		
	13	1452				5	88		1	6		
	14	1166	3			49	64		8	4		-28
	15	767				84	16		20	1		-21
	16	476	81					1	17			
	17	120			70			10			19	

2,4-Dimethyl-3-thiapentane

A vibrational analysis of this compound by digital computer was undertaken as an aid in identifying the fundamental vibrational frequencies in the observed molecular spectra. The procedure differed somewhat from that used in the calculations for tetramethyllead. Most of the observed bands of tetramethyllead were initially assigned, and the calculations were made to obtain estimates of the unassigned fundamentals. In those calculations, initial values for the force constants were refined to give the best least-squares agreement between observed and calculated wavenumbers. For 2,4-dimethyl-3-thiapentane, on the other hand, most of the observed bands were initially unassigned and could not be used in the calculation, so an approximate set of force constants was used to calculate wavenumbers for the 51 fundamental vibrations. Values of the force constants simply were selected by reference to vibrational analyses for structurally related molecules. The set of calculated wavenumbers obtained with those values of the force constants, when compared with the observed spectra, then served as a useful guide in assigning observed wavenumbers to the fundamental vibrations.

The equilibrium configuration of 2,4-dimethyl-3-thiapentane was assumed to be that shown in Figure 20. In this configuration, the molecule has C_2 point group symmetry. Since the molecule contains 21 atoms, there are $3(21) - 6 = 57$ internal degrees of freedom, of which 51 are vibrational modes and 6 are internal rotational modes (4 methyl rotations and 2 isopropyl rotations). The internal degrees of freedom are distributed by sym-

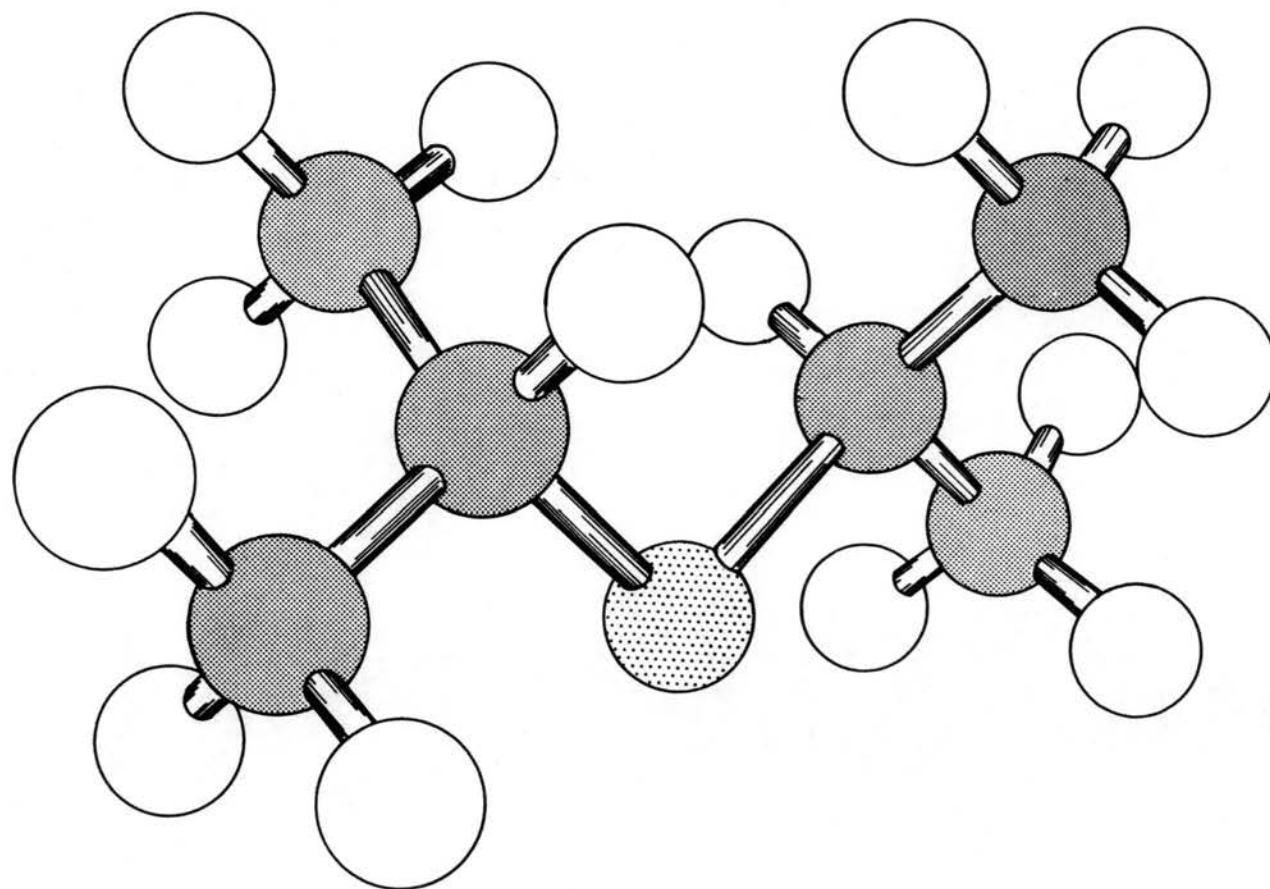


Figure 20 - Equilibrium Configuration of 2,4-Dimethyl-3-thiapentane

metry species as: total, 29A + 28B; vibrational, 26A + 25B; internal rotational, 3A + 3B. All 51 vibrational frequencies to be assigned from the observed spectra are allowed by selection rules in both the Raman and infrared spectrum.

Since there are no degenerate vibrations, the symmetry coordinates are easily written down by inspection, and so are not included here.

The potential energy expression was a Urey-Bradley force field, supplemented by three trans-angle-bending interaction constants. The force constants and their values are given in Table XXV.

The force constants involving the sulfur atom (K_{CS} , H_{CSC} , F_{CSC} , etc.) were transferred from "overlay" calculations for methanethiol and 2-thiopropane (31), with the exception of H_{CCS} and F_{CCS} , which were estimated. In the "overlay" calculations, the set of force constants was found that gave the best agreement between calculated and observed wavenumbers for the two compounds just mentioned. The value used for $K_{CH(CH)}$ was that of Schachtschneider and Snyder (32), rounded to two significant figures. The remaining force constants were transferred from "overlay" calculations for ethane, propane, and cyclohexane (33). The results of the calculation made with the values in Table XXV are given in Table XXVI.

The force constants obtained from the "overlay" calculations for methanethiol and 2-thiopropane were used by Scott and Kruse (36) to estimate the wavenumbers of the fundamental vibrations of 2-propanethiol. For each vibration of the C_3H_7S group in 2-propanethiol, there will be two vibrations for $C_3H_7SC_3H_7$. The two may have the same frequency, or they may be

split by several wavenumbers, but in either case, the two will not be drastically different from the value for 2-propanethiol. The vibrational assignment for 2-propanethiol is known with some confidence, and the differences between observed and calculated wavenumbers for that molecule should be a rough estimate of the differences between observed and calculated wavenumbers for 2,4-dimethyl-3-thiapentane. This was taken into account in assigning the observed wavenumbers given in Table XXVI to the corresponding calculated values.

Table XXVI lists only the bands assigned to fundamentals. The assignment was fairly straightforward with the aid of the calculated wavenumbers and with the aid of the observed wavenumbers for 2-propanethiol. One exception was the value for the C-S-C bending mode, calculated to be 141 cm^{-1} . The band observed at 74 cm^{-1} in the infrared spectrum of the vapor seems to be too low for this mode and is assigned to one of the isopropyl torsional modes. A very weak band has been observed at 155 cm^{-1} in the Raman spectrum of the liquid, although this band was not reported by the original investigators (34). This band may be due to the C-S-C bending vibration, but the vapor-state value for this vibration is still not determined from the spectra. The wavenumber for this vibration was estimated from the experimental thermodynamic properties to be about 129 cm^{-1} , as shown in the next chapter. This indicates a frequency shift of about $20 - 30 \text{ cm}^{-1}$ between liquid and vapor states. This shift is not unreasonable in view of some of those previously encountered.

Table IX, page 23, lists the bands observed for 2,4-dimethyl-3-thiapentane in the far infrared region. Weak bands interpreted as combination or overtone bands were observed at 330, 476, 604, and 620 cm^{-1} in the liquid spectrum and at 474 and 610 cm^{-1} in the vapor spectrum. None of these bands appear in the solid-state spectrum.

TABLE XXV

FORCE CONSTANTS FOR 2,4-DIMETHYL-3-THIAPENTANE
(K and F in units of md A^{-1} ; H, f^{\dagger} , and χ in md A rad^{-2})

Force Constant	Value	Force Constant	Value
$K_{\text{CH}} (\text{CH}_3)$	4.483	F_{CCH}	0.534
$K_{\text{CH}} (\text{CH})$	3.900	F_{CCS}	0.500
K_{CC}	1.931	F_{CSC}	-0.238
K_{CS}	1.854	F_{SCH}	0.640
H_{HCH}	0.550	F_{CCC}	0.531
H_{CCH}	0.331	$\chi (\text{CH}_3)$	0
H_{CCS}	0.500	$\chi (\text{CH})$	0
H_{CSC}	1.644	$f_{\gamma}^{\dagger *}$	0.100
H_{SCH}	0.156	$f_{\gamma\omega}^{\dagger **}$	0.114
H_{CCC}	0.531	$f_{\gamma\omega}^{\dagger ***}$	0.100
F_{HCH}	0		

* C-C-C and C-C-H trans interaction, C-C common

** C-C-S and C-C-H trans interaction, C-C common

*** C-C-H and C-C-H trans interaction, C-C common

TABLE XXVI
OBSERVED AND CALCULATED WAVENUMBERS OF
2,4-DIMETHYL-3-THIAPENTANE

obs ^a	calc	Δ	obs ^a	calc	Δ
	141 A		1054 ^b R(p)	1073 A	-19
290 R(p) IR	270 A	20	1094 R(?) IR	1086 B	8
306 IR	313 B	-7	1118 R(?) IR	1104 A	14
354 R(?) IR	{ 360 B	-6	1150 R(?) IR	{ 1155 A	-5
	{ 361 A	-7		{ 1157 B	-7
426 R(p) IR	396 A	30	1236 IR	1250 B	-14
432 IR	410 B	22	1248 R(p) IR	1248 A	0
650 R(p) IR	{ 656 A	-6	1295 IR	1302 B	-7
	{ 660 B	-10	1311 R(?) IR	1309 A	2
880 R(p) IR	{ 860 A	20	1364 IR	1387 A & B	-23
	{ 862 B	18	1380 R(?) IR	1391 A & B	-11
925 R(?) IR	{ 920 B	5	1450 R(?) IR	1462 4A&4B	-12
	{ 928 A	-3	2864 R(p) IR	2871 2A&2B	-7
948 R(?) IR	{ 963 B	-15	2914 ^c R(p) IR	2912 A & B	2
	{ 964 A	-16	2959 R(?) IR	2980 4A&4B	-21
1042 R(d) IR	1071 B	-29			

^aThe Raman data are from Reference (34). The infrared data are from Reference (35) and from this research. The values below 500 cm^{-1} are for the vapor state, and the remaining values are for the liquid state.

^bThe 1059 cm^{-1} infrared band disappears in the solid-state spectrum and is therefore not assigned to a fundamental.

^cMean of the Fermi-resonance doublet at 2906-2922 cm^{-1} in the Raman Spectrum.

CHAPTER IV

STATISTICAL THERMODYNAMIC APPLICATIONS

The experimental determination of the thermodynamic properties of a compound at only a few temperatures usually takes months to complete. The ability to calculate these properties at temperatures outside the range of experimental data is of obvious importance. The usual procedure is to calculate the thermodynamic properties to the harmonic-oscillator, rigid-rotator approximation from spectroscopic and molecular structure data at the temperatures at which experimental data are available. This gives a check on the vibrational assignment and allows determination of structural parameters, if necessary. Comprehensive tables of the thermodynamic properties are then prepared by calculating the properties at many temperatures.

Obviously, the correct assignment of the fundamental vibrational frequencies of the molecule is requisite for the statistical thermodynamic calculations. If the molecule has low-frequency vibrations, it is almost a must to determine the vapor-state wavenumbers of these by far infrared spectroscopy, since, as was shown in Chapter II, the liquid-state values are more often than not different from the vapor-state values.

Tetramethyllead

Resolution of the Entropy Discrepancy. - This investigation has led to a new vibrational assignment for tetramethyllead, given in Chapter III. The reason for suspecting the unreliability of the previous assignments was that the calculated entropy did not agree with the observed value in the vapor state, $100.48 \pm 0.20 \text{ cal deg}^{-1} \text{ mole}^{-1}$ at 298.15°K (37). For example, Lippincott and Tobin (25) calculated with their vibrational assignment, $S^\circ = 99.86 \text{ cal deg}^{-1} \text{ mole}^{-1}$. In their calculation, Lippincott and Tobin assumed free rotation of the methyl groups, and any hindrance of the methyl groups would make the discrepancy between the observed and calculated entropy values even greater.

Figure 14 shows that the wavenumber of the \underline{f}_2 C-Pb-C bending mode is 120 cm^{-1} for the vapor state. This is significantly different from the value used by previous investigators, so it is evident why earlier assignments, which based the \underline{f}_2 frequency on liquid-state spectra, did not give the correct calculated vapor-state entropy.

Although we now have an accurate value for the \underline{f}_2 C-Pb-C bending frequency, the far infrared spectrum gives no information about the \underline{e} mode, which is infrared inactive. Some binary combinations involving the \underline{e} frequency are allowed by selection rules in the infrared, but no observed band could definitely be assigned to such a combination. However, with the assurance that the correct entropy would be calculated with the correct vapor-state frequencies, we can use the observed entropy value to calculate the wavenumber for the \underline{e} C-Pb-C bending frequency. In the treatment

that follows, vibrational anharmonicity is neglected and rotation of the methyl groups is assumed free.

We calculate the contribution to the entropy of all other vibrational, translational, rotational, and free internal rotational degrees of freedom, and when this is subtracted from the observed entropy, the remaining entropy should be due to the \underline{e} C-Pb-C bending vibration. The contribution of the translational, rotational, and free internal rotational degrees of freedom to the entropy at 298.15°K is 79.74 cal deg⁻¹ mole⁻¹. A normal-coordinate calculation was made in order to obtain values for the \underline{e} and \underline{f}_1 modes for use in calculating the contribution to the entropy of all vibrations except the \underline{e} C-Pb-C bending mode. This vibrational contribution is 14.44 cal deg⁻¹ mole⁻¹. This leaves 6.30 cal deg⁻¹ mole⁻¹ to be accounted for by the \underline{e} mode, and from this the value 117 ± 6 cm⁻¹ was calculated for the \underline{e} mode, the uncertainty of 6 cm⁻¹ corresponding to an uncertainty of 0.20 cal deg⁻¹ mole⁻¹ in the experimental entropy.

The value found here for the \underline{e} C-Pb-C bending frequency was used in the normal-coordinate calculations described in Chapter III. The value is a maximum one, because if the rotation of the methyl groups is hindered at all, a lower wavenumber would be calculated for the \underline{e} mode from the observed entropy. For example, if the barrier hindering rotation of the methyl groups is assumed equal to RT at room temperature, 592 cal mole⁻¹, the calculated wavenumber would be 104 cm⁻¹. However, free or nearly-free internal rotation of the methyl groups is reasonable. Recent unpublished studies

of infrared bandwidth phenomena by Jones and Sheppard (38) at Cambridge University suggest strongly that the barrier hindering rotation of the methyl groups in tetramethyllead is considerably less than RT . Also, a low barrier is suggested by the position of lead in the periodic table with respect to carbon and silicon. The methyl barrier has been determined to be about $4.5 \text{ kcal mole}^{-1}$ in tetramethylmethane (39) and $1.6 \text{ kcal mole}^{-1}$ in tetramethylsilane (8).

A wavenumber for the \underline{e} C-Pb-C bending mode very close to that for the \underline{f}_2 mode (120 cm^{-1}) is also reasonable, since the observation of a single Raman band suggests that the two frequencies are nearly the same in the liquid. Also, failure to detect binary combinations involving the \underline{e} mode may only mean that they nearly coincide with binary combinations involving the \underline{f}_2 mode and so are not observed separately.

Table XXI shows that the wavenumbers calculated for the \underline{e} and \underline{f}_1 vibrations are very nearly the same as for the same types of vibration of species \underline{f}_2 . Therefore, in the absence of significant non-Urey-Bradley interactions that would make the calculated \underline{e} wavenumbers differ from the present ones, we would not expect to resolve the \underline{e} and \underline{f}_2 bands in the Raman spectrum.

Thermodynamic Properties.-The thermodynamic properties of tetramethyllead were calculated to the rigid-rotator, harmonic-oscillator, independent-internal-rotator approximation, with the usual formulas of statistical thermodynamics (40). For these calculations, the molecular parameters given on page 66 were used. With these parameters, the three equal principal moments of inertia were de-

terminated to be $3.61 \times 10^{-38} \text{ g cm}^2$, and the reduced moment of inertia for internal rotation of a single methyl group was determined to be $5.32 \times 10^{-40} \text{ g cm}^2$. The vibrational contributions were calculated with the vibrational assignment given in Table XXIII.

Table XXVII gives values at several temperatures of the Gibbs energy function, enthalpy function, enthalpy, entropy, heat capacity, enthalpy of formation, Gibbs energy of formation, and the logarithm of the equilibrium constant of formation. The value of the enthalpy of formation at 298.15°K was taken from reference (37), and the values of the thermodynamic functions of carbon, hydrogen, and lead were taken from the JANAF Tables (41).

TABLE XXVII

THE MOLAL THERMODYNAMIC PROPERTIES OF TETRAMETHYLLEAD IN THE IDEAL GAS STATE

T °K	$(\underline{G}^\circ - \underline{H}_0^\circ)/T$ cal deg ⁻¹	$(\underline{H}^\circ - \underline{H}_0^\circ)/T$ cal deg ⁻¹	$\underline{H}^\circ - \underline{H}_0^\circ$ kcal	\underline{S}° cal deg ⁻¹	\underline{C}_p° cal deg ⁻¹	$\underline{\Delta H_f}^\circ$ kcal	$\underline{\Delta G_f}^\circ$ kcal	log $\underline{K_f}^\circ$
0	0	0	0	0	0	40.5	40.5	infinite
273.15	-75.4	22.2	6.06	97.6	32.3	33.2	62.0	-49.6
298.15	-77.4	23.1	6.89	100.5	34.1	32.6	64.7	-47.4
300	-77.5	23.2	6.96	100.7	34.3	32.6	64.9	-47.3
400	-84.7	26.9	10.7	111.6	41.4	30.5	76.0	-41.5
500	-91.0	30.4	15.2	121.4	47.4	28.9	87.6	-38.3
600	-96.9	33.7	20.2	130.6	52.6	27.5	99.4	-36.2
700	-102.3	36.7	25.7	139.0	57.1	25.2	111.7	-34.9
800	-107.4	39.5	31.6	146.9	61.0	24.3	124.2	-33.9
900	-112.2	42.1	37.9	154.3	64.5	23.6	136.7	-33.2
1000	-116.7	44.5	44.5	161.2	67.6	23.2	149.3	-32.6

*The standard enthalpy and Gibbs energy, and common logarithm of the equilibrium constant of formation by the reaction, $4C(c, \text{graphite}) + 6H_2(g) + Pb(c \text{ or } l) = C_4H_{12}Pb(g)$. The reference states for lead are the crystals above the dotted line and the liquid below.

2,4-Dimethyl-3-thiapentane

Conformational Analysis.—Unpublished calorimetric studies of this compound have been made in the Thermodynamics Laboratory of the Bartlesville Petroleum Research Center. Experimental values of the entropy at three temperatures, the vapor heat capacity at five temperatures, and the heat of formation at 298.15°K, all corrected to the ideal gas state, were determined.

Table XXVI gives the vibrational assignment for 2,4-dimethyl-3-thiapentane, with the exception of the C-S-C bending mode. It was stated in Chapter III that the vapor-state wavenumber for this vibration could not be determined from the spectra. Therefore, this wavenumber was one of the parameters that had to be estimated from the experimental thermodynamic properties.

Figure 20 shows one possible configuration of 2,4-dimethyl-3-thiapentane. Other configurations are possible by rotation of the isopropyl groups. If the potential barrier hindering rotation of each isopropyl group has a minimum every $2\pi/3$ radians, that is at each staggered position, there would be nine "rotational isomers." For moderate energy differences between nonequivalent isomers, the change in relative amounts with temperature would contribute to the heat capacity. The temperature dependence of the observed heat capacity is not what would be expected from such equilibria among conformations with moderate energy differences. Seven of the conformations involve close approach of methyl groups, and it is likely that the potential energy of these forms is quite high. In that case, they are present in con-

centrations so small that equilibria involving them have a negligible effect on the thermodynamic functions. The two remaining conformations are optical isomers, one of which is shown in Figure 20. It is noteworthy that the thermodynamic properties of 3-thiapentane have also been interpreted on the basis that the high energy (C_s) form does not contribute significantly to the thermodynamic functions (42).

Since a molecule with 21 atoms is quite complex for theoretical calculations, some approximations were made to simplify the calculations and reduce the number of structural parameters that had to be determined.

One of the assumptions that was made was that the potential barrier hindering rotation of the methyl groups in 2,4-dimethyl-3-thiapentane is the same as that in 2-propanethiol. The value $4.0 \text{ kcal mole}^{-1}$ was used for 2,4-dimethyl-3-thiapentane. This is the rounded value of the barrier obtained from the thermodynamic properties of 2-propanethiol.

Another assumption made in treating this molecule was that the torsional mode in which the isopropyl groups move out of phase, which gives rise to the infrared band observed at 74 cm^{-1} in the vapor spectrum, could be treated as a harmonic oscillation.

With the assumptions made above, the contributions to the thermodynamic functions of translation, rotation, vibration (except for the C-S-C bending mode), the methyl rotations, the unsymmetrical isopropyl rotation, and the mixing of optical isomers, can be calculated. This leaves the contribution of the C-S-C bending vibration and the symmetrical isopropyl rotation to be

accounted for. The total contribution of these two modes is the difference between the observed value and the contributions listed above. The interpretation for these two modes must be consistent with the three entropy and five heat capacity values. The value 155 cm^{-1} can be used as the wave-number for the C-S-C bending vibration to estimate the heat capacity contribution of this vibration, since this contribution changes very little ($0.01 - 0.02 \text{ cal deg}^{-1} \text{ mole}^{-1}$) in the temperature range of interest as the value for the frequency changes to reasonable values. Therefore, the remaining heat capacity is due to the symmetrical isopropyl rotation. Since the d- and l- optical isomers are changed into one another by this rotation, the potential barrier hindering the motion can probably be treated as a double-minimum barrier. The potential function used to calculate the contribution of the symmetric isopropyl rotation to the thermodynamic functions consists of two cosine-shaped wells separated by a constant-energy barrier. This potential function is shown in Figure 21.

The method for calculating the thermodynamic properties due to this potential function is similar to that described by Scott and McCullough (43). The ratio d/D and V were adjusted to give the best agreement with the observed heat capacity. After the best values of d/D and V were found, the entropy calculated with these values at the temperatures of the experimental data were added to the previously calculated entropy contributions. The remaining differences between observed and calculated entropy values were assigned to the C-S-C bending vibration. The values of the parameters found

in this way are:

$$d/D = 1/2$$

$$V = 1780 \text{ cal mole}^{-1}$$

$$\nu (\text{C-S-C bend}) = 129 \text{ cm}^{-1}$$

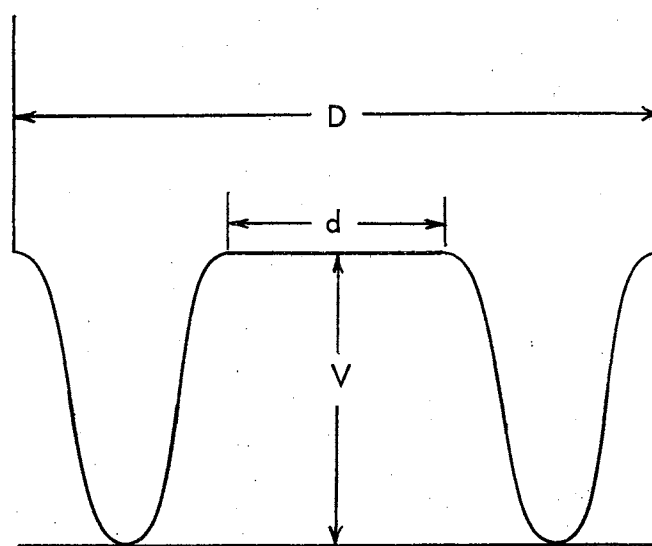


Figure 21 - Potential Function Assumed for Isopropyl Rotation

Table XXVIII shows the agreement between observed and calculated entropy and heat capacity values. The deviations in the table lie well within the experimental uncertainty. This shows that the thermodynamic properties can be interpreted on the basis of the two optical isomers being the only conformations present in appreciable concentration.

TABLE XXVIII

COMPARISON OF OBSERVED AND CALCULATED ENTROPY AND
HEAT CAPACITY FOR 2,4-DIMETHYL-3-THIAPENTANE

entropy (cal deg ⁻¹ mole ⁻¹)				heat capacity (cal deg ⁻¹ mole ⁻¹)			
T(°K)	obs	calc	Δ	T(°K)	obs	calc	Δ
349.57	106.21	106.14	0.07	380.2	48.83	48.76	0.07
369.83	108.81	108.80	0.01	405.2	51.10	51.11	-0.01
393.16	111.69	111.77	-0.08	433.2	53.59	53.63	-0.04
				464.2	56.28	56.29	-0.01
				500.2	59.18	59.23	-0.05

Thermodynamic Properties. - The thermodynamic properties of 2,4-dimethyl-3-thiapentane in the ideal gas state were calculated. The bond distances and angles that were used are: C-C, 1.53 Å; C-H, 1.10 Å; C-S, 1.82 Å; C-S-C, 98°52'; all other angles, tetrahedral.

The average reduced moment of inertia of the methyl groups was calculated by the method of Kilpatrick and Pitzer (44) to be 5.29×10^{-40} g cm², and the contributions of the hindered methyl rotations to the thermodynamic properties were obtained from the tables of Pitzer and Gwinn (11).

Table XXIX gives the molal thermodynamic properties of 2,4-dimethyl-3-thiapentane.

TABLE XXIX

THE MOLAL THERMODYNAMIC PROPERTIES OF 2,4-DIMETHYL-3-THIAPENTANE IN
THE IDEAL GAS STATE

T	$(\underline{G}^\circ - \underline{H}^\circ_0)/T$	$(\underline{H}^\circ - \underline{H}^\circ_0)/T$	$\underline{H}^\circ - \underline{H}^\circ_0$	\underline{S}°	\underline{C}_p°	$\Delta\underline{H}_f^{\circ*}$	$\Delta\underline{G}_f^{\circ*}$	$\log \underline{K}_f^*$
$^\circ\text{K}$	cal deg^{-1}	cal deg^{-1}	kcal	cal deg^{-1}	cal deg^{-1}	kcal	kcal	
0	0	0	0	0	0	-39.85	-39.85	infinite
273.15	-72.59	23.23	6.345	95.82	38.22	-48.68	-7.03	5.62
298.15	-74.68	24.59	7.332	99.27	40.71	-49.27	-3.18	2.33
300	-74.84	24.69	7.407	99.53	40.90	-49.32	-2.89	2.11
400	-82.66	29.97	11.99	112.64	50.63	-51.47	12.92	-7.06
500	-89.90	34.98	17.49	124.88	59.22	-53.18	29.22	-12.77
600	-96.70	39.64	23.78	136.33	66.40	-54.48	45.83	-16.69
700	-103.13	43.91	30.74	147.04	72.45	-55.43	62.63	-19.55
800	-109.24	47.82	38.25	157.06	77.61	-56.04	79.55	-21.73
900	-115.10	51.35	46.22	166.45	82.02	-56.42	96.50	-23.43
1000	-120.67	54.63	54.63	175.30	85.88	-56.51	113.52	-24.81

* The standard enthalpy and Gibbs energy, and common logarithm of the equilibrium constant of formation by the reaction, $6\text{C}(\text{c, graphite}) + 7\text{H}_2(\text{g}) + 1/2 \text{S}_2(\text{g}) = \text{C}_6\text{H}_{14}\text{S}(\text{g})$.

BIBLIOGRAPHY

1. Blaine, L. R., E. K. Plyler, and W. S. Benedict, J. Research Natl. Bur. Standards, 66A, 223 (1962).
2. Yaroslavskii, N. G., and A. E. Stanwich, Optika i Spektroskopiya, 5, 384 (1958).
3. Yost, D. M., D. W. Osborne, and C. S. Garner, J. Am. Chem. Soc., 63, 3492 (1941).
4. Scott, D. W., G. B. Guthrie, J. F. Messerly, S. S. Todd, W. T. Berg, I. A. Hossenlopp, and J. P. McCullough, J. Phys. Chem., 66, 911 (1962).
5. Scott, D. W., W. N. Hubbard, J. F. Messerly, S. S. Todd, I. A. Hossenlopp, W. D. Good, D. R. Douslin, and J. P. McCullough, J. Phys. Chem., 67, 680 (1963).
6. Scott, D. W., W. D. Good, G. B. Guthrie, S. S. Todd, I. A. Hossenlopp, A. G. Osborn, and J. P. McCullough, J. Phys. Chem., 67, 685 (1963).
7. Fateley, W. G., I. Matsubara, and R. E. Witkowski, Spectrochim. Acta, in press.
8. Scott, D. W., J. F. Messerly, S. S. Todd, G. B. Guthrie, I. A. Hossenlopp, R. T. Moore, Ann Osborn, W. T. Berg, and J. P. McCullough, J. Phys. Chem., 65, 1320 (1961).
9. Green, J. H. S., W. Kynaston, and H. M. Paisley, J. Chem. Soc., 1963, 473.
10. Kilb, R. W., Tables of Mathieu Eigenvalues and Eigenfunctions for Special Boundary Conditions, I and II, Department of Chemistry, Harvard University.
11. Pitzer, K. S., and W. D. Gwinn, J. Chem. Phys., 10, 428 (1942).

12. Stejskal, E. O., and H. S. Gutowsky, J. Chem. Phys., 28, 388 (1958).
13. McCullough, J. P., H. L. Finke, D. W. Scott, M. E. Gross, J. F. Messerly, R. E. Pennington, and Guy Waddington, J. Am. Chem. Soc., 76, 4796 (1954).
14. Hubbard, W. N., D. R. Douslin, J. P. McCullough, D. W. Scott, S. S. Todd, J. F. Messerly, I. A. Hossenlopp, Ann Osborn, and Guy Waddington, J. Am. Chem. Soc., 80, 3547 (1958).
15. Hubbard, W. N., H. L. Finke, D. W. Scott, J. P. McCullough, C. Katz, M. E. Gross, J. F. Messerly, R. E. Pennington, and Guy Waddington, J. Am. Chem. Soc., 74, 6025 (1952).
16. Costain, C. C., Personal Communication to D. W. Scott.
17. Wilson, E. B., J. C. Decius, and P. C. Cross, "Molecular Vibrations," McGraw-Hill Book Company, Inc., New York, N. Y., 1955.
18. King, W. T., Ph. D. Thesis, University of Minnesota, 1956.
19. Overend, J., and J. R. Scherer, J. Chem. Phys., 32, 1289 (1960).
20. Duncan, A. B. F., and J. W. Murray, J. Chem. Phys., 2, 146 (1934); ibid., 636.
21. Young, C. W., J. S. Koehler, and D. S. McKinney, J. Am. Chem. Soc., 69, 1410 (1947).
22. Siebert, H., Z. anorg. u. allgem. Chem., 263, 82 (1950); 268, 177 (1952); 271, 75 (1952).
23. Sheline, R. K., and K. S. Pitzer, J. Chem. Phys., 18, 595 (1950).
24. Hall, R. W., Ph. D. Thesis, University of Oklahoma, 1952.
25. Lippincott, E. R., and M. C. Tobin, J. Am. Chem. Soc., 75, 4141 (1953).
26. Jackson, J. A., Jr., Ph. D. Thesis, University of Oklahoma, 1955.
27. Shimizu, K., J. Chem. Soc. Japan, Pure Chem. Sect., 77, 1284 (1956).
28. Waters, D. N., and L. A. Woodward, Proc. Roy. Soc. (London), A246, 119 (1958).
29. Overend, J., and J. R. Scherer, J. Opt. Soc. Am., 50, 1203 (1960).

30. Wong, C., and V. Schomaker, J. Chem. Phys., 28, 1007 (1958).
31. Scott, D. W., and F. H. Kruse, Unpublished Results.
32. Schachtschneider, J. H., and R. G. Snyder, Spectrochim. Acta, 19, 117 (1963).
33. Scott, D. W., and F. H. Kruse, Unpublished Results.
34. American Petroleum Institute Research Project 44 at the Texas A and M University, Catalog of Raman Spectral Data, Serial No. 374.
35. American Petroleum Institute Research Project 44 at the Texas A and M University, Catalog of Infrared Spectral Data, Serial Nos. 1465, 2026, 2027, 2198, 2443, 2444.
36. Scott, D. W., and F. H. Kruse, Unpublished Results.
37. Good, W. D., D. W. Scott, J. L. Lacina, and J. P. McCullough, J. Phys. Chem., 63, 1139 (1959).
38. Sheppard, N., Personal Communication to D. W. Scott. For an account of the method see: Jones, W. J., and N. Sheppard, Proc. Chem. Soc. (London), 420 (1961).
39. Aston, J. G., "A Treatise on Physical Chemistry," I, eds. H. S. Taylor and S. Glasstone, D. Van Nostrand Company, Inc., New York, N. Y., 1942, p. 597.
40. Pitzer, K. S., "Quantum Chemistry," Prentice-Hall, Inc., Englewood Cliffs, N. J., 1953, Chapters 7 and 9.
41. JANAF Thermochemical Tables, prepared under the auspices of the Joint Army-Navy-Air Force Thermochemical Panel at the Thermal Laboratory, the Dow Chemical Company, Midland, Michigan, D. R. Stull, Project Director.
42. Scott, D. W., H. L. Finke, W. N. Hubbard, J. P. McCullough, G. D. Oliver, M. E. Gross, C. Katz, K. D. Williamson, Guy Waddington, and Hugh M. Huffman, J. Am. Chem. Soc., 74, 4656 (1952).
43. Scott, D. W., and J. P. McCullough, Bureau of Mines Report of Investigations 5930, 1962.
44. Kilpatrick, J. E., and K. S. Pitzer, J. Chem. Phys., 17, 1064 (1949).

VITA

Gene A. Crowder

Candidate for the Degree of

Doctor of Philosophy

Thesis: FAR INFRARED SPECTRA AND THEIR APPLICATION TO SELECTED
PROBLEMS OF MOLECULAR ENERGETICS

Major Field: Physical Chemistry

Biographical:

Personal Data: Born in Wichita Falls, Texas, October 25, 1936, the son of Raymond M. and Jewel M. Crowder.

Education: Graduated from Blanchard High School, Blanchard, Oklahoma, in 1954; received the Bachelor of Science degree from Central State College in May, 1958; received the Master of Science degree from the University of Florida in August, 1961; completed requirements for the Doctor of Philosophy degree in August, 1964.

Professional experience: Assistant Research Chemist, Petroleum Chemicals, Inc., Lake Charles, La., 1958 - 1959; graduate research assistant, University of Florida, 1959 - 1961; Petroleum Research Fund Fellow, Oklahoma State University, 1961 - 1964.

Membership in Professional Organizations: American Chemical Society; American Association for the Advancement of Science; Alpha Chi Sigma.